Synthesis of π-conjugated block copolymer containing poly(3-hexylthiophene) and bent-core liquid crystal

So Ryong Lim

Department of Molecular Science

(Chemistry)

Graduate School of UNIST

Synthesis of π-conjugated block copolymer containing poly(3-hexylthiophene) and bent-core liquid crystal

So Ryong Lim

This certifies that the thesis of So Ryong Lim is approved.

01. 00. 2016 Month/Day/Year of submission

signature

_____

Ja-Hyoung Ryu

signature

_____

Kyoung Taek Kim

signature

_____

Sung You Hong

Abstract

Synthesis of π-conjugated block copolymer containing poly(3-hexylthiophene) and spontaneous bent-core liquid crystal., 2016, So Ryong LIM, Graduate Program of Chemistry, Ulsan National Institute of Science and Technology (UNIST).

Conjugated polymers consist of organic macromolecules, of which the polymer backbones are comprised of alternating double- and single-bonds. Conjugated polymers have high conductivity and chemical stability due to an overlap of π-molecular orbitals. Conjugated polymer-based materials have various advantages such as lightweight, low cost, flexibility, and processability. Polythiophene (PT) is an important conjugated polymer. PT has excellent thermal stability, environmental stability, and good conductivity, but has poor solubility. To improve the solubility of PT, flexible side chains were attached onto the backbone. Poly(3-alkylthiophene) (P3AT) can dramatically improve the solubility. The properties of a conjugated polymer are strongly dependent on the morphology of the material in the solid-state.

The aim of study was to investigate the morphologies formed self-assembly of block copolymers containing P3HT. We synthesized ethynyl-terminated P3HT by Grignard Metathesis polymerization (GRIM method) and characterized it. The ethynyl-terminated P3HT was reacted with azide-terminated PS or PEG via Cu(I)-catalyzed cycloaddition (click chemistry). The self-assembly behavior of P3HT-*b*-PS in a thin film was studied by treating the thin films with solvent annealing using chloroform or toluene as a solvent. The self-assembly behavior of P3HT-*b*-PEGs in aqueous solution was studied. The resulting block copolymers self-assembled into nanofibers in solution presumably due to the crystallization of the core-forming P3HT block.

Liquid crystals (LCs) are materials in a state that has properties between those of a conventional liquid and those of a solid crystal. Bent-core LCs have special features of the LC phases formed by banana-shaped molecules (with a bend angle of ~120°). The well-defined morphologies of bent-core LC have exotic physicochemical properties.

We synthesized two chiral bent-core mosogens (P8-O-PIMB6* and P9-O-PIMB7*) and an achiral bent-core mesogen (P8-O-PIMB6) in order to obtain well-defined morphologies in the 60 nm AAO nanochannel. The structures of bent-core mesogens were confirmed by NMR and EI-mass spectrometry.

The transition temperatures of bent-core mesogens were measured by DSC. The morphologies of bent-core liquid crystals in the 60 nm AAO nanochannel were studied by depolarized reflected light microscopy (DRLM), scanning electron microscopy (SEM), and grazing incidence X-ray diffraction (GIXD).

Contents

List of Tables

List of Schemes

List of Figures

VIII

List of Abbreviation

AAO	Anodic Aluminum Oxide
AFM	Atomic-force microscopy
bPEG	branched Poly(ethylene glycol)
n-BuLi	n-Butyllithium
DCC	*N,N'*-Dicyclohexylcarbodiimide
DCM	Dichloromethane
DIAD	Diisopropyl azodicarboxylate
DLS	Dynamic light scattering
DMAP	4-Dimethylaminopyridine
DMF	*N,N'*-dimethylformamide
DRLM	Depolarized reflected light microscopy
DSC	Differential scanning calorimetry
EA	Ethyl acetate
EtOH	Ethyl alcohol
GIXD	Grazing incidence X-ray diffraction
GPC	Gel permeation chromatography
GRIM	Grignard metathesis
HCl	Hydrochloric acid
HH	Head-to-head
HT	Head-to-tail
Hx	Hexane
LC	Liquid crystal
LDA	Lithium diisopropylamide
MALDI-TOF	Matrix-assisted laser desorption/ionization-Time of flight
MeOH	Methyl alcohol
Mn	Number average molecular weight
Mw	Weight average molecular weight
MWCO	Molecular weight cutoff
NaOH	Sodium hydroxide
Ni(dppp)Cl2	Dichloro(1,3-bis(diphenylphosphino)propane)nickel
NMR	Nuclear magnetic resonance
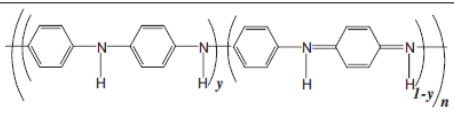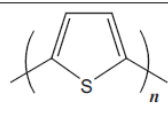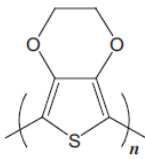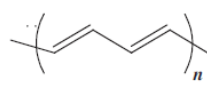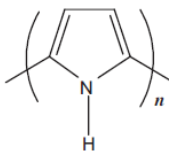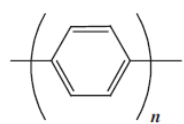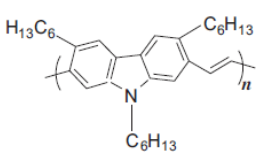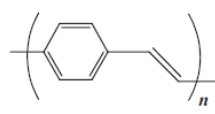
PDI	Polydispersity index
PEG	Poly(ethylene glycol)
PMDETA	*N,N,N',N'',N''*-penta methyldiethylenetriamine
P3HT	Poly(3-hexylthiophene)
PS	Polystyrene
PT	Polythiophene
rrP3AT	Regioregular poly(3-alkylthiphene)
SEM	scanning electron microscopy
TEA	Triethylamine
TEM	Transmission electron microscopy
THF	Tetrahydrofuran
TT	Tail-to-tail

1. Introduction

1.1 π-Conjugated polymer

  The discovery of highly conductive polyacetylene by Heeger, Shirakawa, and MacDiarmid attracted great interest to π-conjugated polymers as organic conducting or semiconducting materials[1]. π-Conjugated polymers consist of organic macromolecules, of which the polymer backbones are comprised of alternating double- and single-bonds. Because of the fact that the single and double bonds become similar, double-bonds overlap over the single bonds. Moreover, the π-electrons can easily move from one bond to the other, which makes conjugated polymers regarded as one-dimensional semiconductors[2-3]. Inorganic conductors and semiconductors are more efficient than their organic counterparts. However, they are associated with issues like high cost of production, scarcity of materials, and toxicity. Because of these problems associated with inorganic conductors and semiconductors, organic electronic materials have attracted attention as low cost and solution-processable alternatives[4]. One of the most interesting properties of π-conjugated polymers is that they possess excellent processability. The chemical structures of the most important π-conjugated polymers are presented in Table 1.1.

Table 1.1 Chemical structures of typical π-conjugated polymers[3].

1.2 Poly(3-alkylthiophenes) (P3ATs)

Polythiophene (PT) is an important π-conjugated polymer, which was first chemically prepared in the early 1980s by a metal-catalyzed polycondensation polymerization of the mono-Grignard of 2,5-dibromothiophene generated by treatment with magnesium metal[5-6]. However, PT has poor solubility due to the strong π-stacking interactions between the aromatic rings[7]. Nevertheless, PTs have excellent thermal stability, environmental stability, and good conductivity[8]. Soluble PTs with flexible side chains, poly(3-alkylthiophene)s (P3ATs) were synthesized by Elsenbaumer et al. for 2,5-coupled polythiophene[9]. It has been demonstrated that the attachment of flexible side chains onto the backbone of an insoluble polymer can dramatically improve the solubility.
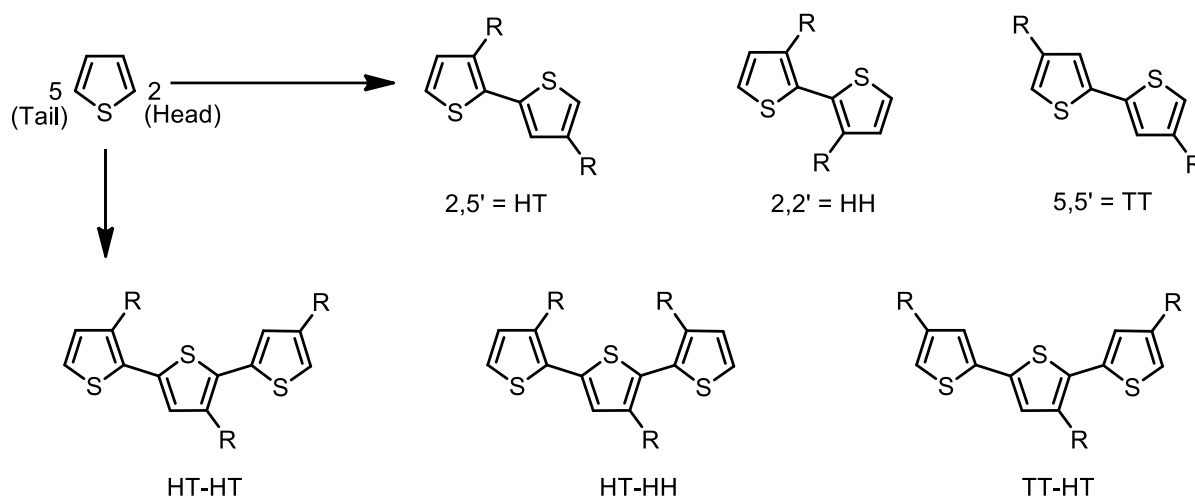
Figure 1.1 Classical synthetic methods lead to a number of regiochemical isomers[10].

However, the coupling of 3-alkythiophenes to synthesize P3ATs suffers from the random coupling yielding region-irregular polymers which possess 50-80% head-to-tail (HT) microstructures along the backbone[11-12] (Figure 1.1). The loss of regioregularity is due to multiple head-to-head (HH) and tail-to-tail (TT) couplings, which cause a sterically twisted structure in the polymer backbone, giving rise to a loss of π-conjugation. Steric twisting of backbones leads to the destruction of high conductivity and other desirable properties for PTs[13] (Figure 1.2).

2
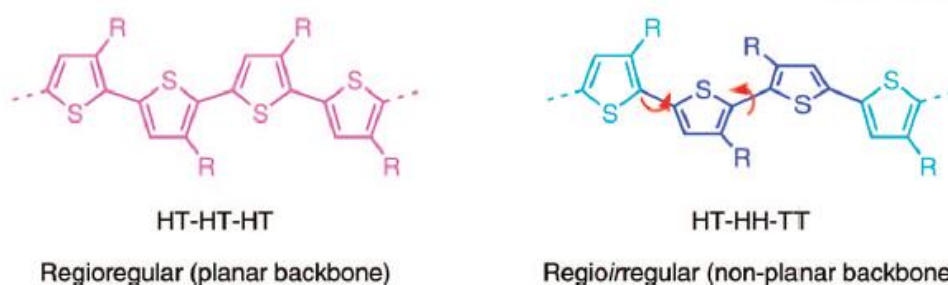
Figure 1.2 Regioregular P3AT (rrP3AT) and regioirregular P3AT. (Reprinted with permission from Itaru Osaka, Richard D. McCullough, Advances in Molecular Design and Synthesis of Regioregular Polythiophenes, Accounts of Chemical Research. Copyright (2008) American Chemical Society)[14].

Generally, regioregular P3AT (rrP3AT) is synthesized by three methods commonly referred to as the McCullough[15-16], Rieke[17-18], and GRIM methods[19]. These methods all produce comparable P3ATs in terms of regioregularity. However, the Rieke method offers the advantage of being tolerant to a variety of different functional groups, whereas McCullough and GRIM are limited to those that are tolerant to organolithium and organomagnesium reagents. The McCullough method is known as the first synthesis method of HT rrP3AT. Lithiation of 2-bromo-3-alkylthiophenes, using lithium diisopropylamide (LDA) at cryogenic temperatures followed by transmetalation with $MgBr_2 \cdot Et_2O$ generates 2-bromo-5-(bromomagnesio)-3-alkylthiophene. This intermediate is then polymerized with $Ni(dppp)Cl_2$ to give PATs with 98-100% HT-HT couplings. The second synthetic approach to HT-PAT was subsequently described by Rieke. In this method, Rieke zinc, noted as Zn*, undergoes selective oxidative addition to 2,5-dibromo-3-alkylthiophenes at cryogenic temperatures to afford one regiochemical intermediate. This metalated intermediate undergoes regioselective polymerization to yield the desired HT rrP3AT. In 1999, McCullough et al. described another method to produce regioregular HT-coupled P3AT which can be accomplished at room temperature and at large scale. The Grignard Metathesis reaction (GRIM) entails the treatment of a 2,5-dibromo-3-alkylthiophene monomer with the equivalent of an alkyl Grignard reagent resulting in a magnesiumbromine exchange reaction. Treatment of this intermediate with a catalytic amount of $Ni(dppp)Cl_2$ affords a rrP3AT. The GRIM method is presented in Scheme 2.1.

3
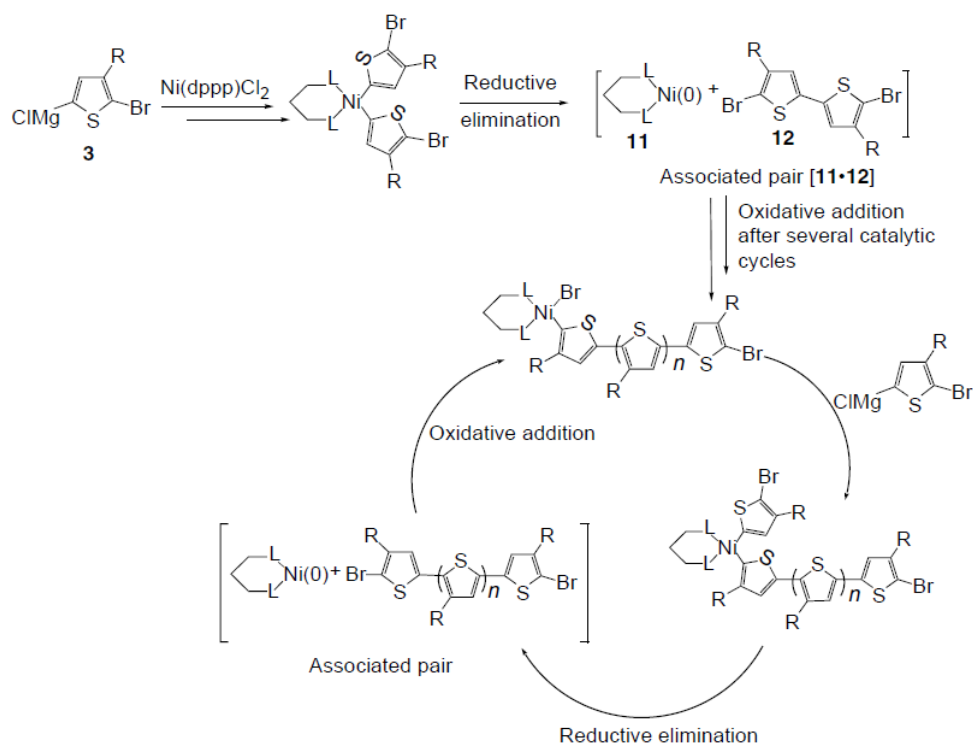
Scheme 1.1 Proposed Mechanism for the Nickel-Initiated Cross-Coupling Polymerization. (Reprinted with permission from Elena E. Sheina, Jinsong Liu, Mihaela Corina Iovu, et al, Chain Growth Mechanism for Regioregular Nickel-Initiated Cross-Coupling Polymerizations, Macromolecules, 2004, 37 (10), 3526-3528. Copyright (2004) American Chemical Society)[20].

1.3 Self-assembly of π-conjugated block copolymer

The properties of a π-conjugated polymer are strongly dependent on the morphology of the material in the solid-state. Block copolymers are known to generate a variety of different morphologies by self-assembly. The self-assembly of π-conjugated block copolymers has been widely used for the creation of nanostructures with the desired shape, size, and physicochemical function.

Poly(3-hexylthiophene)-b-poly(styrene) (P3HT-*b*-PS) films were prepared by casting from toluene. P3HT-*b*-PS self-assembled into well-defined nanowires spaced laterally by 30-40 nm with a length reaching to a few micrometers[21].
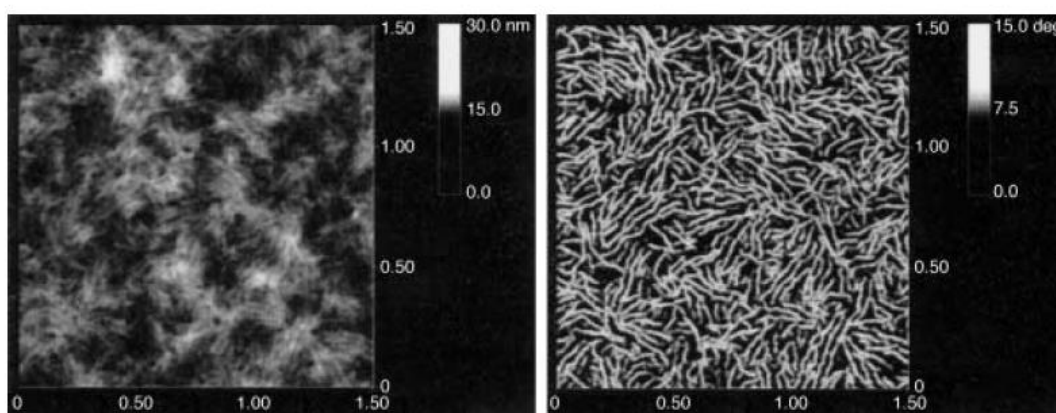
Figure 1.3 nanowire morphology in poly(3-hexylthiophene)-b-poly(styrene) copolymers solvent-cast from toluene and visualized with tapping-mode AFM. Left: height; right: phase. These and subsequent images use gray-scale coding, with darker tones corresponding to lower values (for example, lower heights). (Reprinted with permission from Jinsong Liu, Elena Sheina, Tomasz Kowalewski, Richard D. McCullough, Tuning the Electrical Conductivity and Self-Assembly of Regioregular Polythiophene by Block Copolymerization: Nanowire Morphologies in New Di- and Triblock Copolymers, Angewandte Chemie International Edition, 41 (2), 329-332. Copyright (2002) John Wiley and Sons)[21].

Lin et al. reported that the use of anisole/chloroform mixed selective solvents provides a successful means to control self-assembly of the all-conjugated diblock copolymer poly(3-butylthiophene)-*b*-poly(3-hexylthiophene) (P3BHT) into nanostructured morphologies[22]. The self-assembly structure of The P3BHT was affected by the change in the anisole/chloroform ratio during the cooling (Figure 1.3). P3BHT structure was converted from nanowire to nanoring according to the increase in anisole volume. This result was promoted by the enhanced solvophobic interaction between P3BHT blocks and anisole, thereby minimizing the unfavorable interfacial area per unit volume in the solution.
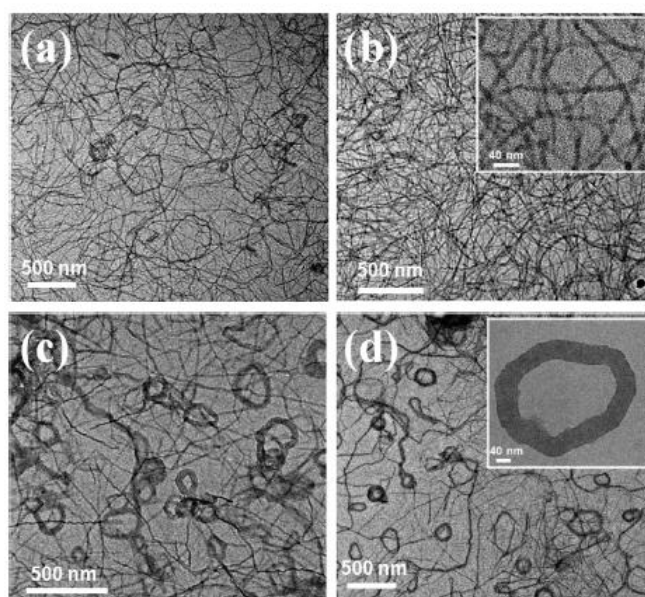
Figure 1.4 TEM images of P3BHT nanostructures self-assembled from the P3BHT anisole/chloroform solutions after cooling from 80 to 10 °C. Nanowires formed from the anisole/chloroform ratio of (a) 1:1 and (b) 2:1 solutions. The average diameter of nanowires is 8_10 nm (inset in b). In addition to nanowires, nanorings appeared in the anisole/chloroform (c) 6:1 and (d) 10:1 solutions. The ring width of a typical nanoring is 50 nm (inset in d). (Reprinted with permission from Ming He, Lei Zhao, Jun Wang, et al., Self-Assembly of All-Conjugated Poly(3-alkylthiophene) Diblock Copolymer Nanostructures from Mixed Selective Solvents. ACS Nano**,** 4 (6), 3241-3247. Copyright (2010) American Chemical Society)[22].

Hayward and coworkers reported a helical nanowires phase in the solution state self-assembly of poly(3-hexylthiophene)-*b*-poly(3-triethylene glycol thiophene) (P3HT-**b**-P3(TEG)T) with added potassium ions[23].
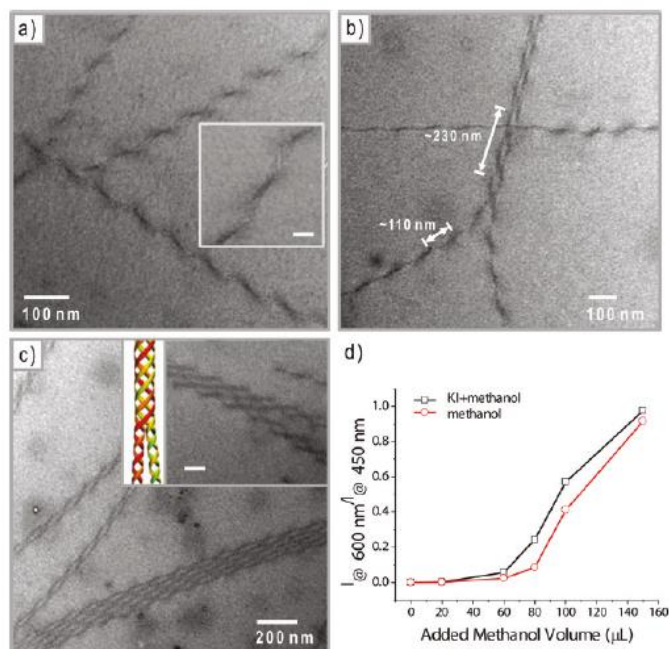
Figure 1.5 (a) TEM images of H2T1 after addition of KI revealed helical ribbons with a regular pitch. Inset: magnified image (scale bar, 20 nm). TEM images showing the structural transformation of H2T1 containing KI (0.47 mM) from (b) single- to double- and (c) multiple-stranded helices. Inset: TEM image and schematic showing association of double helices into quadruple superhelices (scale bar, 100 nm). (d) Absorption changes (monitored at 450 and 600 nm) of H2T1 solution upon gradual addition of methanol, or 0.12 mM KI in methanol, into 200 μL of a chloroform solution of H2T1 (0.1 mg/mL). (Reprinted with permission from Eunji Lee, Brenton Hammer, Jung-Keun Kim, et al., Hierarchical Helical Assembly of Conjugated Poly(3-hexylthiophene)-block-poly(3-triethylene glycol thiophene) Diblock Copolymers, Journal of the American Chemical Society, 133 (27), 10390-10393. Copyright (2011) American Chemical Society)[23].

1.4 Liquid crystal

Liquid crystals (LCs) are materials in a state that has properties between those of a conventional liquid and those of a solid crystal[24]. In other words, LCs have the mobility of liquids and the optical properties of solids. LCs are divided into thermotropic and lyotropic. Thermotropic LCs are prepared by heat, whereas lyotropic LCs are prepared by mixing two or more components. The phases of thermotropic LCs are determined by the molecular arrangements because most molecules constituting the LCs are shaped such as a rod-like structure. The LC phase is divided into two categories, nematic and smectic phase. The molecules exhibiting nematic phase have no positional order, but possess only an orientational order. In other words, the molecules are directed in the same direction. The smectic phases are layered structures that usually occur at slightly lower temperatures than nematic phases. There are many variations of smectic phases. Each layer in smectic A is like a two dimensional liquid, and the long axis of the molecules is typically orthogonal to the layers. They are made up of achiral and nonpolar molecules. As with smectic A, the smectic C phase is layered, but the long axis of the molecules is tilted. Smectic C* phases are smectic phases formed by chiral molecules. This added constraint of chirality causes a slight distortion of the Smectic C structure. Sometimes cholesteric phases are also referred to as chiral nematic phases because they are similar to nematic phases in many regards. Many derivatives of cholesterol exhibit this type of phase.
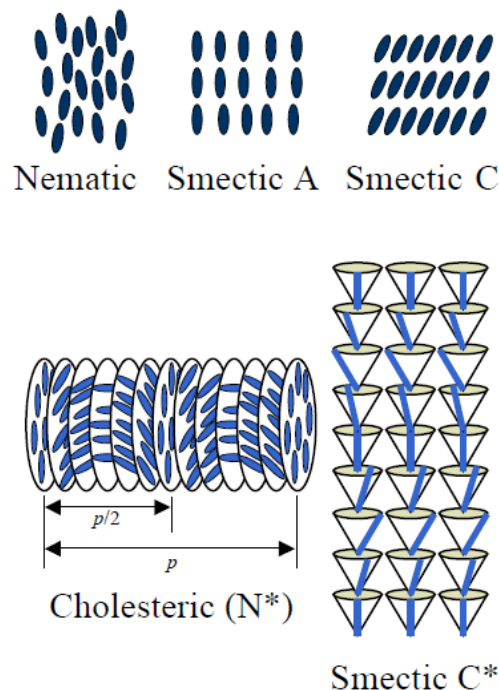
Figure 1.6 Schematic illustration of the different types of liquid crystal phases[26].

8

1.5 Bent-core liquid crystals

Niori et al. reported the unusual ferroelectric behavior of liquid crystals based on achiral bent-core molecules and, so-called "banana-mania" has attractive the field of liquid crystals[25]. Unlike a tranditional rod-like molecular structure, these structures of LC have a bent core within a bend angle of ~120°. In banana mesophases bent-core molecules organize into liquid-like layers but the mesophase character is different from conventional smectic phases in as much as conventional smectic and banana phases are not miscible. The morphologies of bent-core LC are classified from B1 to B7 phases[27] (Figure 1.7). According to this suggestion the smectic high-temperature phase of the pentyloxy and hexyloxy homologs of the parent series is designated as B1. The phase symbol B2 is attributed to the switchable phase of longer-chained homologs whereas the low-temperature phases of the same compounds are designated as B3 or B4. Further smectic phases formed by banana-shaped compounds were given the code letters B5-B7 in the order of their discovery.
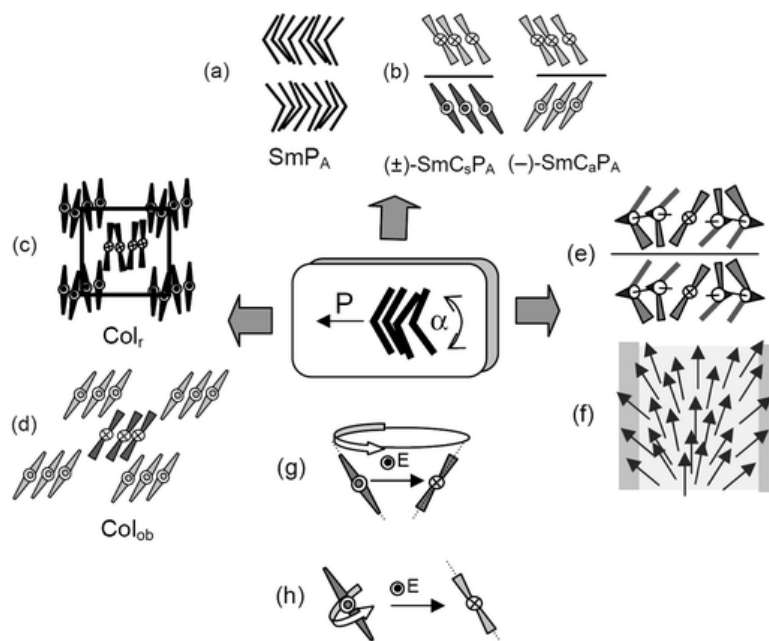
Figure 1.7 Fundamental issues of the organization of bent-core mesogens (P = polar direction, a = bending angle); a) SmP_A = smectic phase with antipolar order (view perpendicular to the polar direction); b) two tilted versions of this mesophase with synclinic (SmC_SP_A) and anticlinic (SmC_AP_A) tilt (views along the polar direction, the grey scale indicates the chirality sense, the SmC_SP_A structure is racemic, the SmC_AP_A structure is homogeneously chiral); c) Colr = rectangular columnar ribbon phase; d) Colob = oblique columnar ribbon phase; e,f) splay of polar direction, e) view along the polar direction, f) view from top, arrows indicate polar directions; g) switching on a cone changes polar direction and tilt

direction and therefore retains the layer chirality; h) switching around the molecular long axes only changes the polar direction and therefore reverses layer chirality. (Reprinted with permission from R. Amaranatha Reddy, U. Baumeister, C. Keith, H. Hahn, H. Lang, C. Tschierske, Influence of the core structure on the development of polar order and superstructural chirality in liquid crystalline phases formed by silylated bent-core molecules: lateral substituents, Soft Matter, 3 (5), 558-570. Copyright (2007) Royal Society of Chemistry) [28].

Some banana mesophases are switchable. They display ferro- and/or antiferroelectric switching behavior[29] (Figure 1.8). Chirality in a tilted SmC phase introduced by chiral dopants or by chirality of the constituting molecules themselves results in a breaking of mirror symmetry. In such chiral tilted phases the symmetry group is reduced. Hence, it permits the appearance of the spontaneous electric polarization in each layer of the SmC* phase.
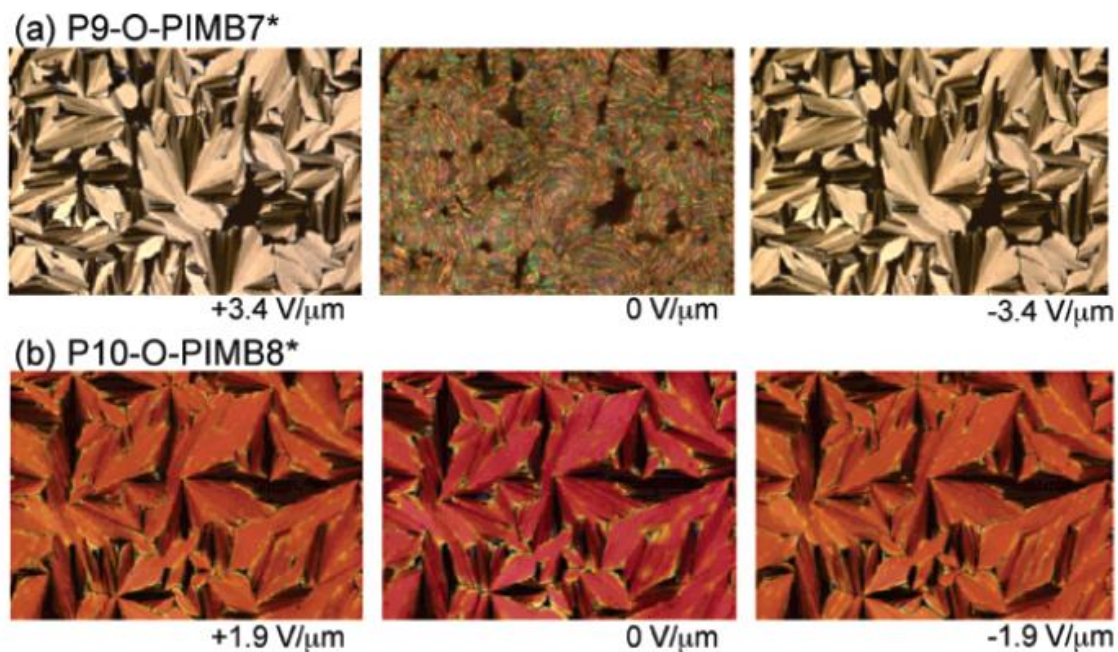
Figure 1.8 Photomicrographs showing the switching behavior in the B2 phase under the application of an electric field. (a) 2.7-μm-thick cell of P9-OPIMB7* at 145 °C. SmC$_S$P$_A$* (E) 0 V μm^{-1}) switches to SmC$_A$P$_F$* under E) (3.4 V μm-1. (b) 5.5-μm-thick cell of P10-O-PIMB8* at 135 °C. SmC$_A$P$_F$* (E) 0 V μm^{-1}) switches to SmC$_A$P$_F$* under the application of an electric field E) (1.9 V μm^{-1}). (Reprinted with permission from Seng Kue Lee, Sung Heo, Jong Gun Lee, et al., Odd−Even Behavior of Ferroelectricity and Antiferroelectricity in Two Homologous Series of Bent-Core Mesogens, 127 (31), 11085-11091. Copyright (2005) American Chemical Society)[29].

1.6 Thesis summary

In Chapter 2, the synthesis and characterization of ethynyl-terminated P3HT are discussed. The synthesis of block copolymers by click chemistry of ethynyl-terminated P3HT and azide-terminated PS and PEG chains is also described. The self-assembly behavior of the resulting block copolymers in bulk and in solution were studied and the nanostructures from self-assembly of the block copolymers were characterized. Chapter 3 summarizes the synthesis of bent-core liquid crystals and the structural characterization of bent-core molecules.

<div align="center">

References

</div>

1. Chiang, C. K.; Fincher, C. R.; Park, Y. W.; Heeger, A. J.; Shirakawa, H.; Louis, E. J.; Gau, S. C.; MacDiarmid, A. G., Electrical Conductivity in Doped Polyacetylene. *Phys. Rev. Lett.* **1977,** *39* (17), 1098-1101.

2. Dubey, N.; Leclerc, M., Conducting polymers: Efficient thermoelectric materials. *J. Polym. Sci., Part B: Polym. Phys.* **2011,** *49* (7), 467-475.

3. Du, Y.; Shen, S. Z.; Cai, K.; Casey, P. S., Research progress on polymer–inorganic thermoelectric nanocomposite materials. *Prog. Polym. Sci.* **2012,** *37* (6), 820-841.

4. Günes, S.; Neugebauer, H.; Sariciftci, N. S., Conjugated Polymer-Based Organic Solar Cells. *Chem. Rev.* **2007,** *107* (4), 1324-1338.

5. Lin, J. W. P.; Dudek, L. P., Synthesis and properties of poly(2,5-thienylene). *J. Polym. Sci.; Polym. Chem. Ed.* **1980,** *18* (9), 2869-2873.

6. Yamamoto, T.; Sanechika, K.; Yamamoto, A., Preparation of thermostable and electric-conducting poly(2,5-thienylene). *J. Polym. Sci. B Polym. Lett. Ed.* **1980,** *18* (1), 9-12.

7. Ballauff, M., Stiff-Chain Polymers—Structure, Phase Behavior, and Properties. *Angew. Chem., Int. Ed.* **1989,** *28* (3), 253-267.

8. Kobayashi, M.; Chen, J.; Chung, T. C.; Moraes, F.; Heeger, A. J.; Wudl, F., Synthesis and properties of chemically coupled poly(thiophene). *Synth. Met.* **1984,** *9* (1), 77-86.

9. Elsenbaumer, R. L.; Jen, K. Y.; Oboodi, R., Processible and environmentally stable conducting polymers. *Synth. Met.* **1986,** *15* (2–3), 169-174.

10. Jen, K.-Y.; Miller, G. G.; Elsenbaumer, R. L., Highly conducting, soluble, and environmentally-stable poly(3-alkylthiophenes). *J. Chem. Soc., Chem. Commun.* **1986,** (17), 1346-1347.

11. Sato, M.; Morii, H., Nuclear magnetic resonance studies on electrochemically prepared poly(3-dodecylthiophene). *Macromolecules* **1991,** *24* (5), 1196-1200.

12. Yokoyama, A.; Miyakoshi, R.; Yokozawa, T., Chain-Growth Polymerization for Poly(3-hexylthiophene) with a Defined Molecular Weight and a Low Polydispersity. *Macromolecules* **2004,** *37* (4), 1169-1171.

13. Chen, T. A.; Rieke, R. D., The first regioregular head-to-tail poly(3-hexylthiophene-2,5-diyl) and a regiorandom isopolymer: nickel versus palladium catalysis of 2(5)-bromo-5(2)-(bromozincio)-3-hexylthiophene polymerization. *J. Am. Chem. Soc.* **1992,** *114* (25), 10087-10088.

14. Osaka, I.; McCullough, R. D., Advances in Molecular Design and Synthesis of Regioregular Polythiophenes. *Acc. Chem. Res.* **2008,** *41* (9), 1202-1214.

15. McCullough, R. D.; Lowe, R. D., Enhanced electrical conductivity in regioselectively synthesized poly(3-alkylthiophenes). *J. Chem. Soc., Chem. Commun.* **1992,** (1), 70-72.

16. McCullough, R. D.; Lowe, R. D.; Jayaraman, M.; Anderson, D. L., Design, synthesis, and control of conducting polymer architectures: structurally homogeneous poly(3-alkylthiophenes). *J. Org. Chem.* **1993,** *58* (4), 904-912.

17. Chen, T.-A.; Wu, X.; Rieke, R. D., Regiocontrolled Synthesis of Poly(3-alkylthiophenes) Mediated by Rieke Zinc: Their Characterization and Solid-State Properties. *J. Am. Chem. Soc.* **1995,** *117* (1), 233-244.

18. Wu, X.; Chen, T.-A.; Rieke, R. D., A Study of Small Band Gap Polymers: Head-to-Tail Regioregular Poly[3-(alkylthio)thiophenes] Prepared by Regioselective Synthesis Using Active Zinc. *Macromolecules* **1996,** *29* (24), 7671-7677.

19. Loewe, R. S.; Khersonsky, S. M.; McCullough, R. D., A Simple Method to Prepare Head-to-Tail Coupled, Regioregular Poly(3-alkylthiophenes) Using Grignard Metathesis. *Adv. Mater.* **1999,** *11* (3), 250-253.

20. Sheina, E. E.; Liu, J.; Iovu, M. C.; Laird, D. W.; McCullough, R. D., Chain Growth Mechanism

for Regioregular Nickel-Initiated Cross-Coupling Polymerizations. *Macromolecules* **2004,** *37* (10), 3526-3528.

21. Liu, J.; Sheina, E.; Kowalewski, T.; McCullough, R. D., Tuning the Electrical Conductivity and Self-Assembly of Regioregular Polythiophene by Block Copolymerization: Nanowire Morphologies in New Di- and Triblock Copolymers. *Angew. Chem., Int. Ed.* **2002,** *41* (2), 329-332.

22. He, M.; Zhao, L.; Wang, J.; Han, W.; Yang, Y.; Qiu, F.; Lin, Z., Self-Assembly of All-Conjugated Poly(3-alkylthiophene) Diblock Copolymer Nanostructures from Mixed Selective Solvents. *ACS Nano* **2010,** *4* (6), 3241-3247.

23. Lee, E.; Hammer, B.; Kim, J.-K.; Page, Z.; Emrick, T.; Hayward, R. C., Hierarchical Helical Assembly of Conjugated Poly(3-hexylthiophene)-block-poly(3-triethylene glycol thiophene) Diblock Copolymers. *J. Am. Chem. Soc.* **2011,** *133* (27), 10390-10393.

24. Reinitzer, F., Contributions to the knowledge of cholesterol. *Liq. Cryst.* **1989,** *5* (1), 7-18.

25. Niori, T.; Sekine, T.; Watanabe, J.; Furukawa, T.; Takezoe, H., Distinct ferroelectric smectic liquid crystals consisting of banana shaped achiral molecules. *J. Mater. Chem.* **1996,** *6* (7), 1231-1233.

26. Larsen, T. T.; Bjarklev, A.; Hermann, D. S.; Broeng, J., Optical devices based on liquid crystal photonic bandgap fibres. *Opt. Express* **2003,** *11* (20), 2589-2596.

27. Pelzl, G.; Diele, S.; Weissflog, W., Banana-Shaped Compounds—A New Field of Liquid Crystals. *Adv. Mater.* **1999,** *11* (9), 707-724.

28. Amaranatha Reddy, R.; Baumeister, U.; Keith, C.; Hahn, H.; Lang, H.; Tschierske, C., Influence of the core structure on the development of polar order and superstructural chirality in liquid crystalline phases formed by silylated bent-core molecules: lateral substituents. *Soft Matter* **2007,** *3* (5), 558-570.

29. Lee, S. K.; Heo, S.; Lee, J. G.; Kang, K.-T.; Kumazawa, K.; Nishida, K.; Shimbo, Y.; Takanishi, Y.; Watanabe, J.; Doi, T.; Takahashi, T.; Takezoe, H., Odd−Even Behavior of Ferroelectricity and Antiferroelectricity in Two Homologous Series of Bent-Core Mesogens. *J. Am. Chem. Soc.* **2005,** *127* (31), 11085-11091.

2. Self-Assembly and Physical Characteristics of π-Conjugated Block Copolymers containing P3HT

2.1 Abstract

  We synthesized terminal alkyne functionalized poly(3-hexylthiophene) (P3HT) by Grignard Metathesis polymerization (GRIM). The polymer was characterized by ^{1}H nucleic magnetic resonance (^{1}H NMR), gel permeation chromatography (GPC), and matrix-assisted laser desorption/ionization-time of flight (MALDI-TOF). We synthesized π-conjugated block copolymer by Cu(I)-catalyzed cycloaddition of ethynyl functionalized P3HT and azide functionalized polystyrene (PS) (P3HT-*b*-PS). The bulk assembly behavior using solvent vapor annealing of the block copolymer was investigated by transmission electron microscopy (TEM). Also, we synthesized amphiphilic block copolymers composed of a hydrophobic P3HT block and a hydrophilic poly(ethylene glycol) (PEG) block. The self-assembly of P3HT-*b*-PEG in aqueous solution was studied by TEM and atomic force microscopy (AFM).

2.2 Introduction

  Semiconducting polymers (π-conjugated polymers) have gained immense interest over the past few years, in part stimulated by their applicability to devices such as organic photovoltaic cells (OPV)[1-2], light emitting diodes[3-4], and field-effect transistors[5-6]. Among the number of π-conjugated polymers, polythiophenes (PTs) are one of the most important and widely studied materials[7-8]. At the initial stage in the history of PTs, unsubstituted polythiophene was prepared through chemical polymerizations. This material was found to be highly conductive and environmentally and thermally stable but had poor solubility[9]. The solubility was improved by substituting alkyl group on PT, called P3AT. P3AT was controlled growth of molecular weight due to improved solubility, and synthesized block copolymer by various methods[10-12].

  McCullough reported the first synthesis of all-polythiophene block copolymers, poly(3-hexylthiophene)-b-poly(3-dodecylthiophene) (P3HT-*b*-P3DD)[13]. Also, McCullough reported nanowire structures formed by self-assembly of poly(3-hexythiophene)-b-polystyrene (P3HT-*b*-PS) by ATRP[14]. Su et al. reported well-defined P3HT block copolymer via the anionic macroinitiation method and self-assembly behavior of poly(3-hexylthiophene)-*b*-poly(2-vinylpridine) (P3HT-*b*-P2VP)[15]. Lin et al.

reported that the use of anisole/chloroform mixed selective solvents provides a successful means to control self-assembly of the all-conjugated diblock copolymer poly(3-butylthiophene)-*b*-poly(3-hexylthiophene) (P3BHT) into nanostructured morphologies[16]. Bielawski et al. synthesized rod-rod block copolymers, Poly(3-hexythiophene)–*b*–poly(g-benzyl L-glutamate) (P3HT-*b*-PBLC) and characterized the morphologies of their self-assembled structures by AFM and TEM[17]. Hayward and coworkers reported helical nanowire structures from the solution self-assembly of poly(3-hexylthiophene)-*b*-poly(3-triethylene glycol thiophene) (P3HT-*b*-P3(TEG)T) in the presence of added potassium ions[18]. Manners et al. reported cylindrical micelles of a controlled length with the polythiophene core via crystallization-driven self-assembly of what block copolymers[19]. Li and co-workers reported a controlled morphology via self-assembly of P3HT blended with F8TBT into nanoaggregates in a mixed solution of O-dichlorobenzene/hexane in order to improve the device performance[20]. Hierarchical self-assembly of amphiphilic poly(3-hexylthiophene)-*b*-poly(ethylene glycol) (P3HT-*b*-PEG) was reported by Park et al[21]. Jenekhe and co-workers reported that poly(3-butylthiophene)-*b*-poly(3-octylthiophene) (P3BT-*b*-P3OT) self-assembled into nanowires in solution[22]. Also, Emrick et al. synthesized P3HT-based diblock copolymer and reported the formation of fibrils by solution self-assembly of the block copolymers, which was studied by TEM[23].

 With an aim to synthesize block copolymers containing a semi-crystalline polythiophene block, we synthesized ethynyl-terminated P3HT by the GRIM method. The synthesized P3HTs were characterized by NMR, GPC, and MALDI-TOF mass spectrometry. The ethynyl-terminated P3HT was reacted with azied-terminated PS or PEG via Cu(I)-catalyzed cycloaddition (click chemistry). The self-assembly behavior of P3HT-*b*-PSs in a thin film was studied by treating the thin films with solvent annealing using chloroform or toluene as a solvent. The morphology of the self-assembled structures of the block copolymer thin films was observed by TEM. By using the same modular synthetic approach, we synthesized amphiphilic diblock copolymers composed of poly(ethylene glycol) and P3HT. The resulting block copolymers self-assembled into nanofibers in solution presumably due to the crystallization of the core-forming P3HT block. The self-assembled structures were studied by DLS, TEM, and AFM.

2.3 Experimental

Materials and Methods

All reagents and chemicals were purchased from commercial sources and used as received. THF was distilled over Na/benzophenone before use. DCM was distilled over CaH_2. All reactions were performed under N_2 unless otherwise noted. NMR spectra were recorded on a Varian VNMRS 600 spectrometer with $CDCl_3$ as a solvent. The molecular weights of block copolymers were measured on a Agilent 1260 Infinity GPC system equipped with a PL gel 5 μm mixed D column (Polymer Laboratories) and differential refractive index detectors. THF was used as an eluent with a flow rate of 1 mL/min. A PS standard (Polymer Laboratories) was used for calibration. MALDI-TOF was performed on a Bruker Ultraflex III TOF-TOF mass spectrometer equipped with a nitrogen laser (335 nm) and operating in a reflectance mode. Internal calibration was performed using a Bruker peptide calibration standard (mass range 1000−4000 Da). The analytical sample was obtained by mixing a THF solution of analyte (30 mg/mL) with a THF solution of matrix (trans-2-[3-(4-ter-butylphenyl)-2-methyl-2-propenylidene] malononitrile (30 mg/mL) as P3HT matrix, sinapinic acid (30 mg/mL) as PS matrix, and silver trifluoroacetate (10 mg/mL)) in a 3/3/1 v/v/v ratio. The prepared solution of the analyte and matrix (0.5 μL) was loaded on the MALDI plate and allowed to dry at room temperature before the plate was inserted into the vacuum chamber of the MALDI instrument. The laser steps and voltages applied were adjusted depending on both the molecular weight and the nature of the analyte. Transmission electron microscopy (TEM) was performed on a JEOL JEM-2100 microscope at an acceleration voltage of 200 kV. Sample specimens were prepared by placing a drop of the solution on a carbon-coated Cu grid (200 mesh, EM science). After 30 min, the solution remaining on the grid was removed with a filter paper, and the grid was air-dried for 24 h. Dynamic light scattering (DLS) experiments were carried out on a BI-200SM equipped with a diode laser (637 nm, 4 mW). All DLS data were handled using Dispersion Technology Software (Brookhaven Instruments). Samples for atomic force microscopy (AFM) measurements were prepared by drop casting a dilute the polymer solution onto precleaned slide glasses, then dried at room temperature for 12 h. AFM images were acquired in tapping mode with a Veeco Series IV Atomic Force Microscope, performed at room temperature under an atmosphere of air using standard silicon cantilevers with a nominal spring constant of 50 N/m and resonance frequency of ~300 kHz. The images were acquired at a scan frequency of 1 Hz over 5×5 μm^2 scan areas.

Synthesis of Ethynyl-terminated Poly(3-hexylthiophene) (P3HT)

Ethynyl-terminated poly(3-hexylthiophene) was synthesized by Grignard Metathesis polymerization (GRIM) following the literature[12]. A 50 mL oven-dried flask was charged with 2,5-dibromo-3-

hexylthiophene (1 g, 3.06 mmol), dry THF (40 mL), and a stir bar. After adding isopropylmagnesium chloride (1.55 mL, 2.0 M solution in THF), the resulting mixture was stirred at ambient temperature for 2 h. Ni(dppp)Cl$_2$ (30.0 mg, 0.055 mmol) (dppp = 1,3-bis(diphenylphosphino)propane) was then added in one portion and the resulting dark orange solution stirred for 10 min. Ethynylmagnesium bromide (1.84 mL, 0.5 M in THF) was then added to the mixture via syringe in one portion. After an additional 5 min of stirring, 80 mL of methanol was poured into the reaction flask, which caused a dark purple solid to precipitate. The solid was isolated via filtration, and then washed with excess methanol and hexanes to remove residual metal salts, unreacted monomer and oligomers, and then dried under vacuum of the desired polymer. ^{1}H NMR (CDCl$_3$, ppm): δ 6.99–6.93 (br, CH thiophene), 3.53–3.46 (s, ethynyl CH), 2.83–2.71 (br, CH$_2$), 1.74–1.51 (br, CH$_2$), 1.44–1.37 (br, CH$_2$), 0.93–0.81 (br, CH$_3$).
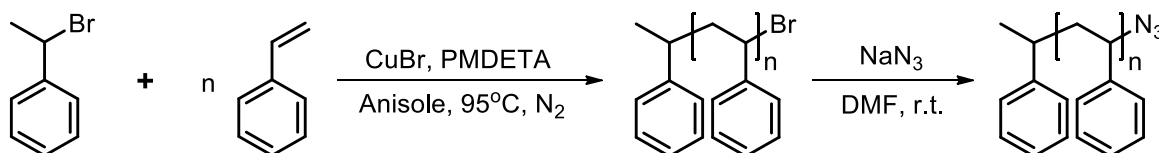
Scheme 2.1 Synthesis of azide-terminated PS.

Synthesis of Azide-terminated Polystyrene (N$_3$-PS)

CuBr (40 mg) was charged in a Schlenk flask and dried in vacuum for 15 min. *N,N,N',N'',N''-penta* methyldiethylenetriamine (PMDETA) (80 mg) dissolved in anisole (1.5 mL) was introduced, and the mixture was stirred under N$_2$ for 15 min. To this mixture, 1-bromoethyl benzene (100 mg, 0.188 mol) and styrene (7 g, 0.0037 mol) dissolved in anisole were added. After the resulting mixture was bubbled with N$_2$ for 15 min, the reaction proceeded at 95 ℃. The reaction was quenched by exposing the solution to air in water bath and diluting it with chloroform. The cooled solution was filtered through a pack of aluminum oxide (basic) with chloroform to remove the Cu catalyst. The filtered solution was concentrated by rotary evaporation, and then crude products were dissolved in a small amount of dichloromethane and precipitated into methanol. White powder was collected by vacuum filtration and dried in vacuo. Subsequently, the brominated PS (1.5 g, 1.4 mmol,) and sodium azide (0.14 g, 2.1 mmol,) were dissolved in DMF (50 mL) and stirred at room temperature. After 10 h, DMF was removed by a rotary evaporator and precipitated into methanol. The azide terminated PS (PS-N$_3$) was dried under vacuum.

A

B
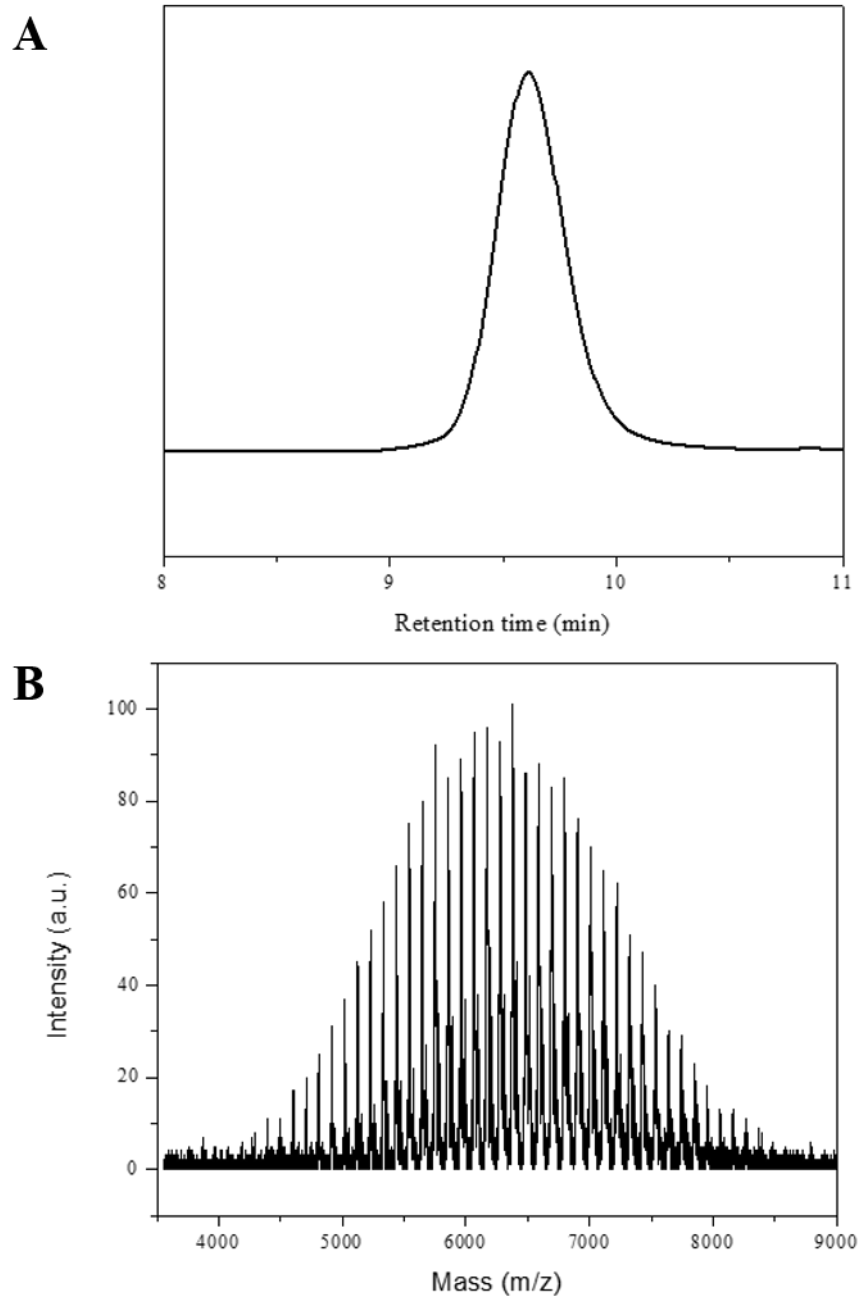
Figure 2.1 GPC data of azide-terminated polystyrene (A) and MALDI-TOF data (B).
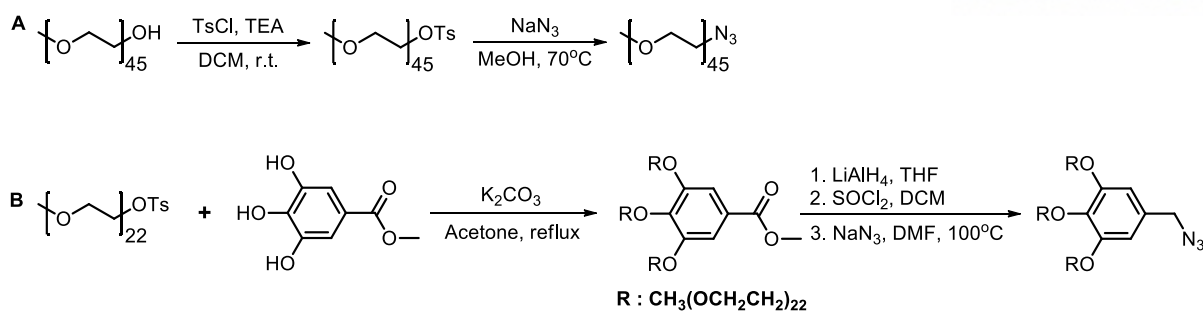
Scheme 2.2 Synthesis of azide-terminated PEG. (A) azide-terminated linear poly(ethylene glycol) (PEG2k-N$_3$). (B) azide-terminated branched poly(ethylene glycol) (bPEG1k-N$_3$).

Synthesis of Azide-terminated linear Poly(ethylene glycol) (N$_3$-PEG2k)

A 1 L Schlenck flask was charged with Poly ethylene glycol methyl ether (Mn = 2000 g/mol, 50 g, 25 mmol), trimethylamine (7.59 g, 75 mmol), and a stir bar. 100 mL dry DCM was dissolved in it. The Schlenk flask was then placed into an ice bath. ρ-toluenesulfonyl chloride (14.30 g, 75 mmol) in 400 mL dry DCM was added dropwise to the Schlenk flask. The reaction mixture was stirred at room temperature for 24 h, and the reaction mixture was then extracted with 1 M HCl. The organic layer was washed with brine and concentrated by rotary evaporation. After removing the solvent, the crude mixture was purified by silica gel column chromatography (DCM/Hx = 95/5, DCM/MeOH = 93/7, v/v). Tosyl terminated PEG (20 g, 10 mmol) and sodium azide (2.6 g, 40 mmol) in dry methanol were refluxed at 70 °C overnight. The reaction mixture was extracted with DCM and washed with brine. The organic layer was dried with MgSO$_4$ and concentrated by rotary evaporator. To well-purified azide terminated PEG, the PEG was precipitated with cold diethyl ether. ^{1}H NMR (CDCl$_3$, ppm): δ 3.78-3.47 (m, CH$_2$CH$_2$), 3.31 (s, CH$_3$).
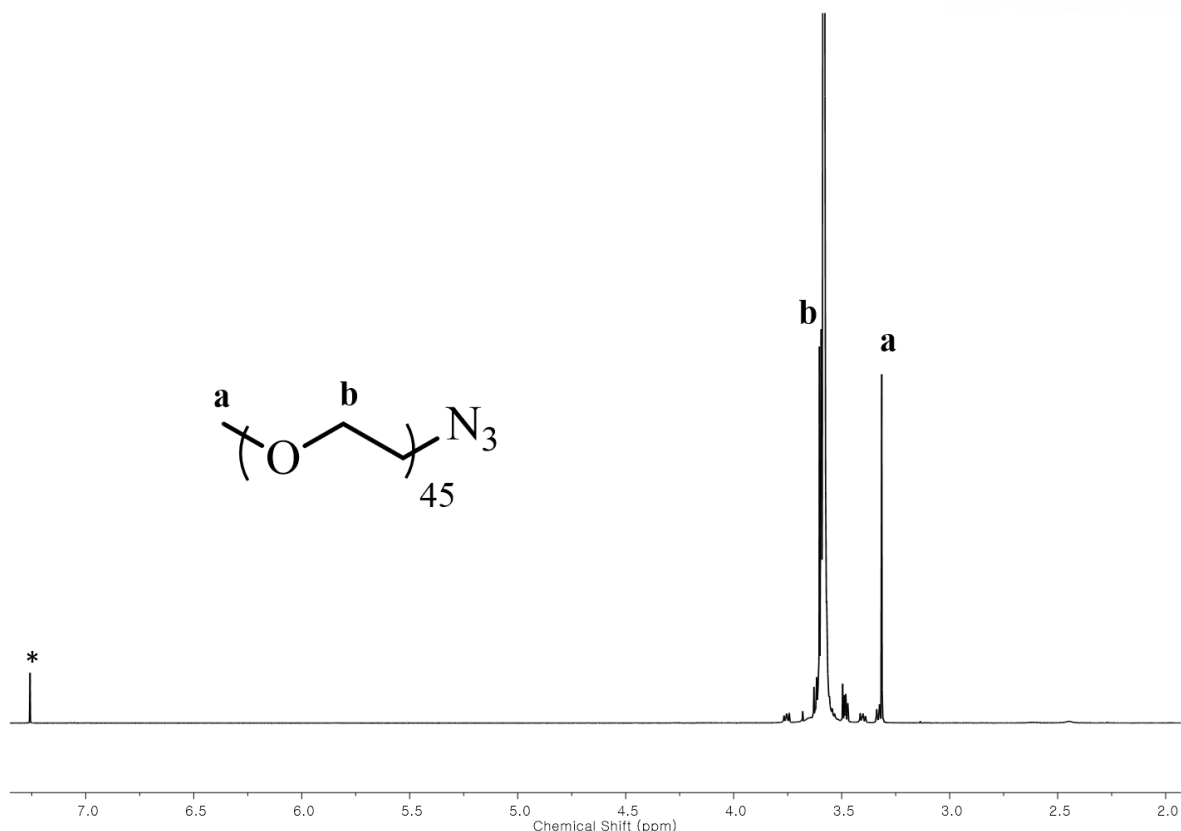
Figure 2.2 ^{1}H NMR spectra of azide-terminated linear poly(ethylene glycol) (PEG2k-N$_3$).

Synthesis of Azide-Terminated branched Poly(ethylene glycol) (N$_3$-bPEG1k)

Branched macroinitiators were synthesized in multi-gram quantity by following the literature methods. A 1 L Schlenck flask was charged with Poly ethylene glycol methyl ether (Mn = 1000 g/mol, 50 g, 50 mmol), trimethylamine (15.18 g, 150 mmol), and a stir bar, into which 100 mL dry DCM was dissolved. The Schlenk flask was then placed into an ice bath. ρ-toluenesulfonyl chloride (28.60 g, 150 mmol) in 400 mL dry DCM was added dropwise to the Schlenk flask. The reaction mixture was stirred at room temperature for 24 h, and the reaction mixture was then extracted with 1 M HCl. The organic layer was washed with brine and concentrated by rotary evaporation. After removing the solvent, the crude mixture was purified by silica gel column chromatography (DCM/Hx = 95/5, DCM/MeOH = 93/7, v/v). A mixture of tosyl terminated PEG (30 g, 25.97 mmol), 3,4,5-trihydroxylbenzoate (1.45 g, 7.87 mmol), K$_2$CO$_3$ (13.05 g, 94.45 mmol) in 250 mL acetone was refluxed for 3 days at 65 °C. The reaction mixture was concentrated by rotary evaporation and dissolved in DCM. The mixture was extracted with 1 M HCl and washed with brine. The organic layer was concentrated on rotary evaporation. After removing the solvent, the crude mixture was purified by silica gel column chromatography (DCM/MeOH = 93/7, v/v). To an ice-cooled suspension of LiAlH$_4$ (0.24 g, 6.29 mmol) in 250 mL dry THF was added

dropwise a solution of the benzoate form PEG (10 g, 3.14 mmol) in 100 mL dry THF. The reaction mixture was allowed to warm to room temperature following the addition. Water was added to the reaction mixture until bubbling stopped and 1 M NaOH was added to the mixture. The reaction mixture was dried with $MgSO_4$ and filtered. The filtered solution was concentrated by rotary evaporation and purified by silica gel column chromatography (DCM/MeOH = 95/5, v/v). To well-purified benzyl alcohol form PEG (5 g, 1.59 mmol) in 100 mL dry DCM was added dropwise thionyl chloride (0.38 g, 3.17 mmol) in 30 mL dry DCM and the mixture was stirred overnight. The reaction mixture was quenched by water and dried $MgSO_4$ and filtered. The organic layer was concentrated by rotary evaporation and purified by silica gel column chromatography (DCM/MeOH = 90/10, v/v). To sodium azide (0.82 g, 12.62 mmol) in anhydrous DMF was added dropwise the benzyl chloride form PEG (4 g, 1.26 mmol) in anhydrous DMF. The mixture was refluxed at 100 °C overnight. The reaction mixture was concentrated by rotary evaporation, extracted with DCM and washed in brine. The organic layer was dried with $MgSO_4$ and concentrated. The mixed compound was purified by silica gel column chromatography (DCM/MeOH = 90/10, v/v). ^{1}H NMR (CDCl$_3$, ppm): δ 6.54 (s, 1H), 4.23 (s, CH$_2$), 4.18-4.11 (m, OCH$_2$), 3.86-3.52 (m, CH$_2$CH$_2$), 3.37 (s, CH$_3$).
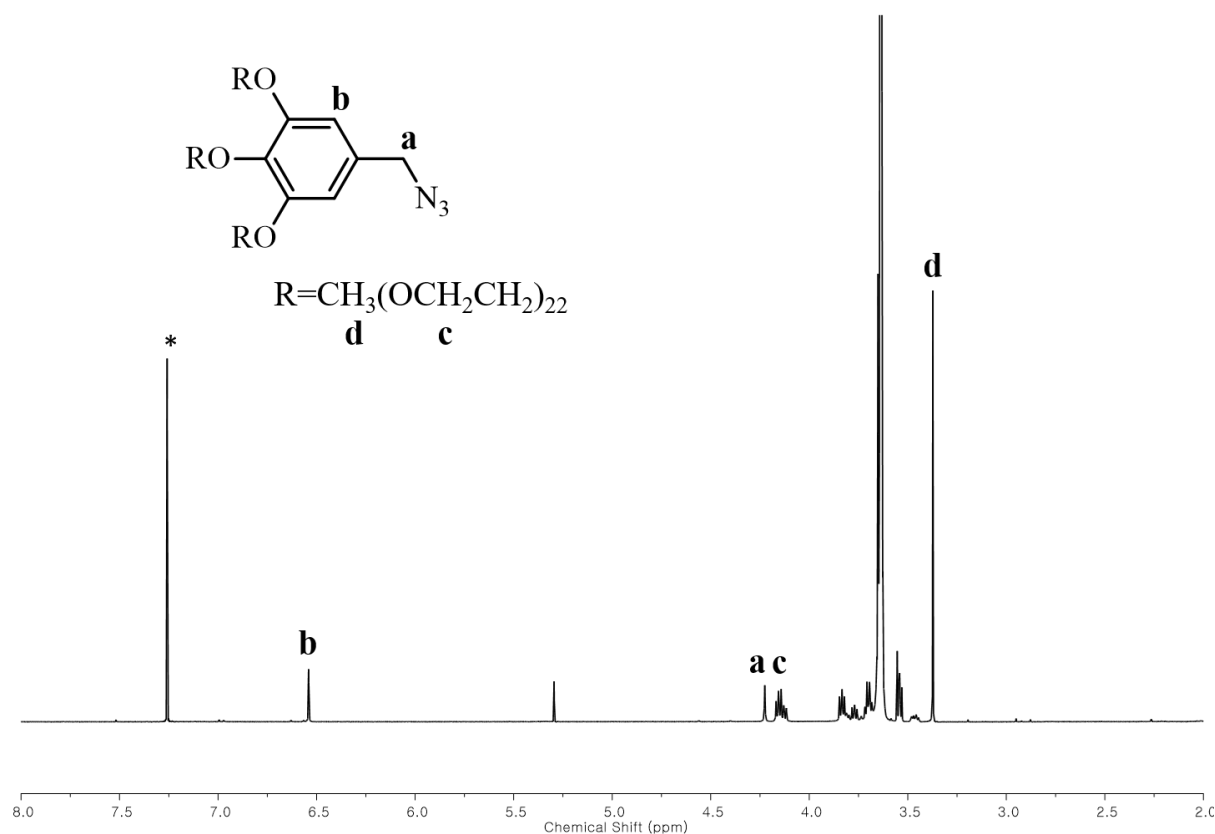
Figure 2.3 ^{1}H NMR spectra of azide-terminated branched poly(ethylene glycol) (bPEG1k-N$_3$).

Synthesis of block copolymer by Copper(I)-catalyzed Azide-Alkyne Cycloaddition (click chemistry)

CuBr (2.73 mg, 0.02 mmol) and *N,N,N',N'',N''*-pentamethyldiethylenetriamine (PMDETA) (3.29 mg, 0.02 mmol) were mixed with 1 mL of THF in a 20 mL Schlenk tube with a magnetic bar. The tube was sealed with a rubber septum. This mixture was bubbled with N_2 for 15 min with gentle stirring. To this solution, a THF solution of ethynyl-terminated P3HT (100 mg, 0.02 mmol) and azide-terminated PS (237.74 mg, 0.04 mmol) was introduced via a syringe. The green solution was degassed by bubbling N_2 for 20 min. After degassing, the tube was immersed in a preheated oil bath (55 °C) and the click reaction was proceeded at this temperature. The progress of the reaction was monitored by taking GPC. When most of the P3HT had reacted with azide-terminated PS, the reaction was quenched by exposing it to air and diluted with $CHCl_3$. The cooled solution was filtered through a pack of basic aluminium oxide with THF to remove the Cu catalyst. The filtered solution was concentrated on a rotary evaporator, and the resulting residue was diluted with THF. This solution was precipitated into methanol and acetone to remove traces of catalyst, ligand, and unreacted azide-terminated PS. Purple powder was collected by vacuum filtration and dried in vacuo. All block copolymers were characterized by ^{1}H NMR and GPC to evaluate the molecular weight and the size distribution.

The block copolymers comprising ethynyl-terminated P3HT and azide-terminated PEG were similarly prepared.

Solvent vapor annealing of P3HT-b-PS

A solution of P3HT-b-PS (0.1 mg/mL) in toluene was dropped on the carbon grid and slowly evaporated. The grid was placed in a closed chamber exposed to toluene and chloroform steam at room temperature for 3 h.

Self-assembly of P3HT-*b*-PEG

The block copolymer (0.2 mg) was dissolved in THF (2 ml) in a 15 ml capped vial with a magnetic stirrer. The solution was stirred for one hour at room temperature. A syringe pump was calibrated to deliver water at a speed of 0.5 mL/h. The vial cap was replaced by a rubber septum. Water (2 mL, MilliQ, 18.2 MV) was added to the organic solution with vigorous stirring (815 revolutions per minute) by a syringe pump with a 6 ml syringe equipped with a steel needle. The resulting suspension solution was subjected to dialysis (molecular weight cutoff (MWCO) 12–14 kDa (SpectraPor)) against water for 24 hours with frequent changes of water.

2.4 Results and Discussion

Block copolymerization
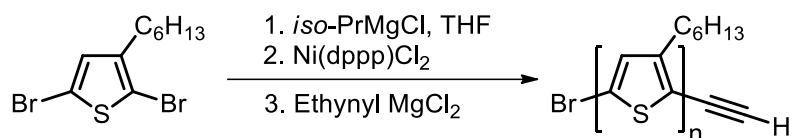
Scheme 2.3 Synthesis of ethynyl-terminated poly(3-hexylthiophene) by GRIM method.

Ethynyl-terminated P3HT was prepared by the GRIM method (Scheme 2.3). Upon storing under ambient condition for ~ 2 weeks, the ethynyl-P3HT produced by the GRIM methods showed significantly reduced solubility and polymer crosslinking presumably due to the reaction between terminal alkynes of the polymer. GPC analysis of the stored ethynyl-P3HT revealed the appearance of a high molecular weight polymer, which was not observed in the as-synthesized sample of ethynyl-P3HT (Figure 2.4). This result suggested that the terminal ethynyl group of the P3HT was unstable and prone to undergo addition under it ambient condition. Therefore, we used P3HT immediately after preparation, or stored under an inert atmosphere in a freezer (~ 2 weeks).
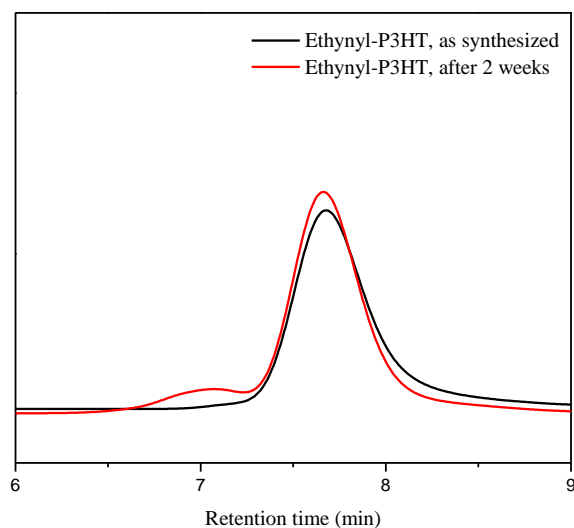
Figure 2.4 GPC data of ethynyl-terminated P3HT.

The ethynyl-terminated P3HT structure was confirmed by ^{1}H NMR, as shown in Figure 2.5. The presence of the ethynyl group of P3HT was confirmed by the peak at 3.5 ppm assigned to the alkyne

proton.
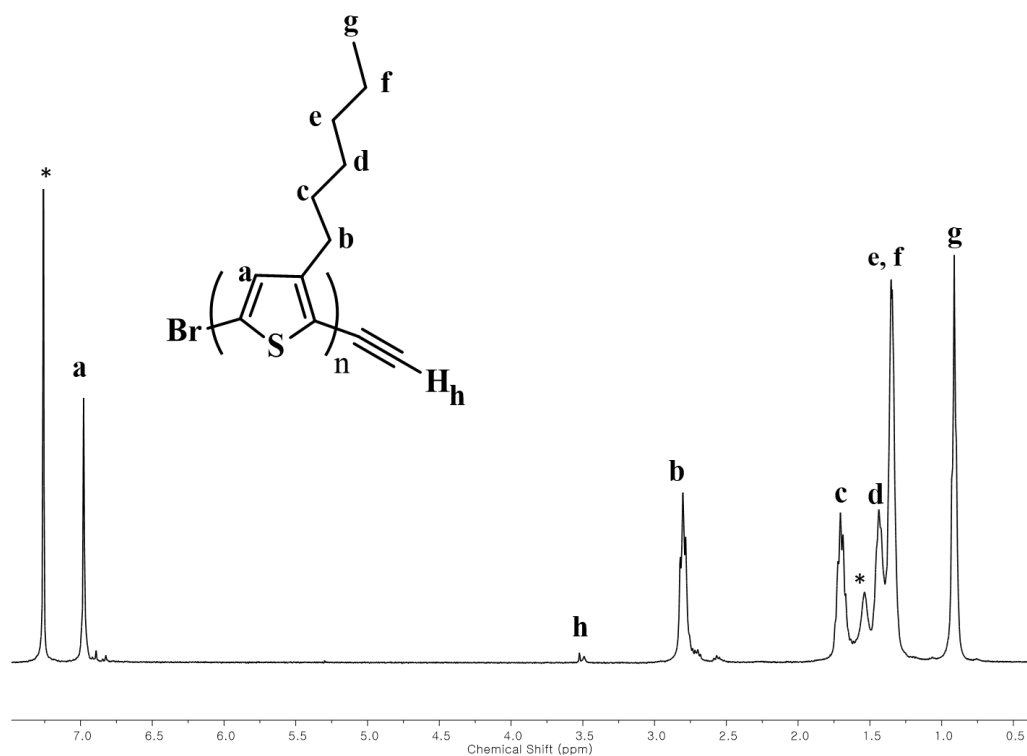
Figure 2.5 ^{1}H NMR spectra of ethynyl-terminated P3HT.

Table 2.1 Characterization of ethynyl-terminated P3HT, azide-terminated PS and PEG, P3HT-*b*-PS, and P3HT-*b*-PEG.

Sample	$[M]_0/[Ni]_0$[a]	Mn (kg/mol)[b]	PDI[b]	Mn (kg/mol)[c]	PDI[c]
1a Ethynyl-P3HT	75/1	9.97	1.10	5.39	1.04
1b Ethynyl-P3HT	50/1	7.85	1.19	3.43	1.11
1c Ethynyl-P3HT	20/1	5.21	1.22	2.55	1.09
2a PS-N3	-	5.97	1.07	6.06	1.01
2b PEG2K-N$_3$	-	2.46	1.06	1.91	1.01
2c bPEG1000-N$_3$	-	3.90	1.05	3.17	1.01
3a (1a+2a)	-	16.81	1.09	-	-
3b (1b+2b)	-	11.48	1.07	-	-
3c (1b+2c)	-	12.26	1.10	-	-
3d (1c+2b)	-	8.27	1.21	-	-
3e (1c+2c)	-	9.13	1.17	-	-

[a] Initial monomer (2,5-dibromo-3-hexylthiophene) to catalyst (Ni(dppp)Cl₂) (dppp = 1,3-bis(diphenylphosphno)propane) ratio.

2 4

The molecular weight of ethynyl-terminated P3HT was measured by GPC and MALDI-TOF (Table 2.1). The molecular weight of ethynyl-terminated P3HTs estimated by GPC was 1.8-2.3 times larger than that measured by MALDI-TOF (Figure 2.6). This overestimation of the molecular weight measured by GPC was attributed to the rigid-rod conformation of P3HT in THF[24], which may increase the polydispersities calculated by MALDI-TOF were identical or slightly lower than those calculated by GPC. This result was explained by the rod-like conformation of ethynyl-terminated P3HT in solution. In spite of the molecular weight difference, GPC and MALDI-TOF mass spectrometry of the P3HT showed almost identical results of polydispersity indices, indicating that the resulting P3HT possessed a narrow size distribution.
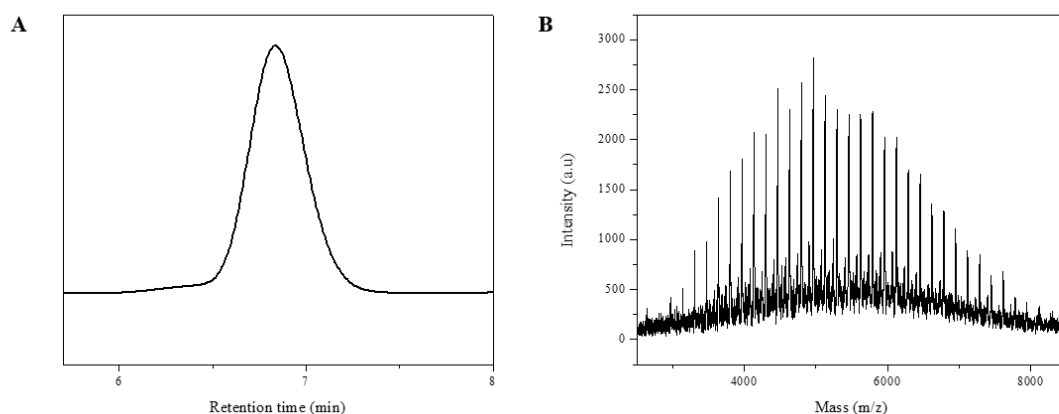
Figure 2.6 GPC date (A) and MALDI-TOF data (B) of ethynyl-terminated P3HT (1a).
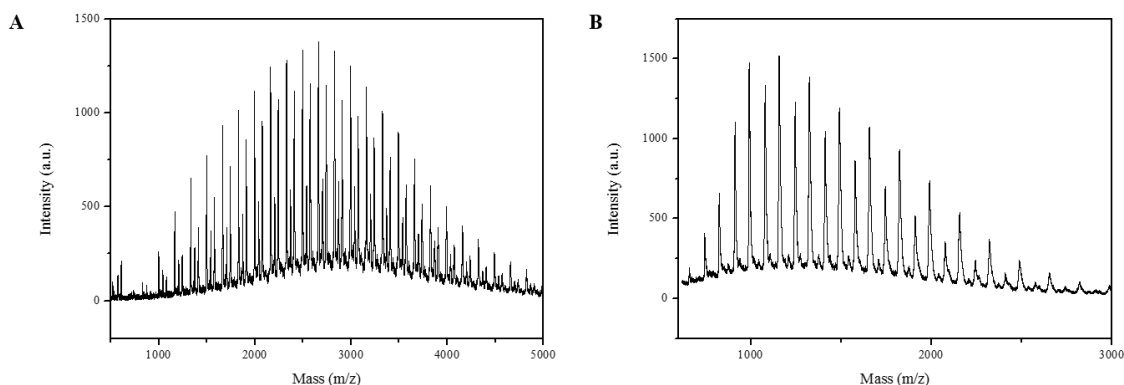
Figure 2.7 MALDI-TOF data of ethynyl-terminated P3HT. (A) 1b and (B) 1c.

2 5
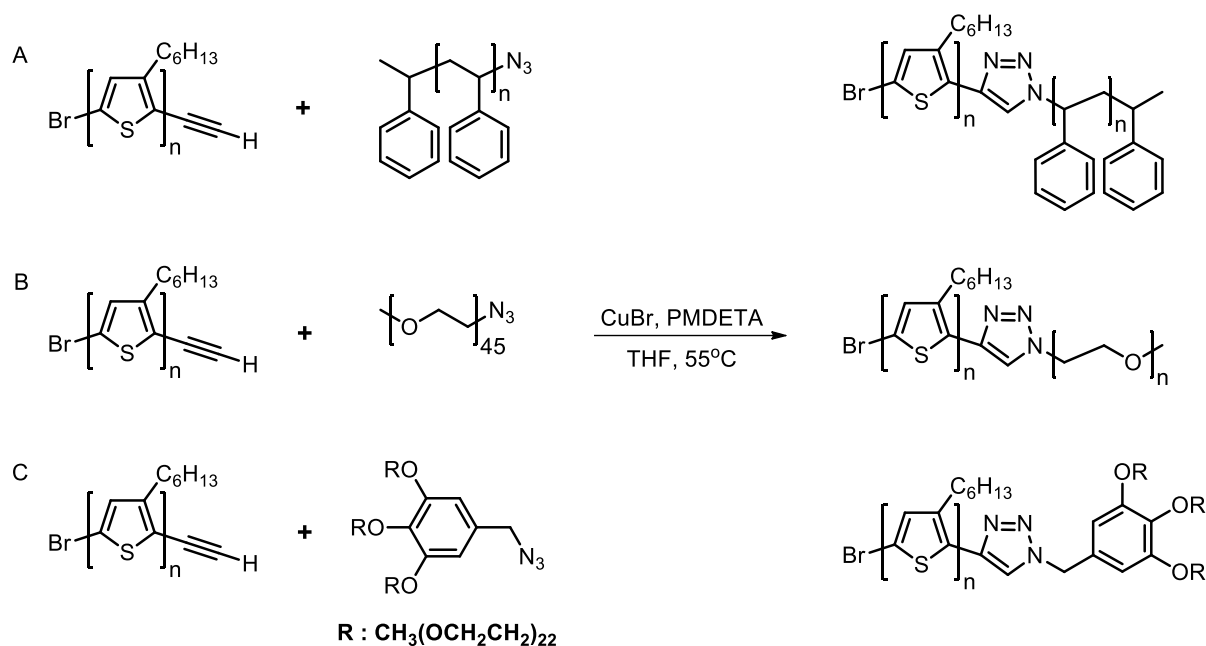
Scheme 2.4 Synthesis of block copolymers containing P3HT by click chemistry. (A) P3HT-*b*-PS. (B) P3HT-*b*-PEG2k. (C) P3HT-*b*-bPEG1k.

The block copolymers of P3HT and a random-coil polymer were synthesized by Cu(I)-catalyzed cycloaddition of a terminal alkyne and azide group of each polymer block (Scheme 2.4). The progress of the cycloaddition was monitored by GPC, which revealed the appearance of the high molecular weight peak during the reaction. After completion, the block copolymers were purified by precipitation using methanol, hexane, and acetone. The GPC result of the purified block copolymer showed a single peak, of which the molecular weight corresponded to the desired block copolymer. The resulting block copolymer were characterized by ^{1}H NMR as shown in Figure 2.8. In the NMR spectra the disappearance of an ethynyl proton of the terminal group of P3HT indicated the successful click reaction. The appearance of the peaks at 7.5 ppm of P3HT-*b*-PS and 7.46 ppm of P3HT-*b*-PEG was attributed to the triazole group formed by the cycloaddition, indicating the formation of the block copolymers.
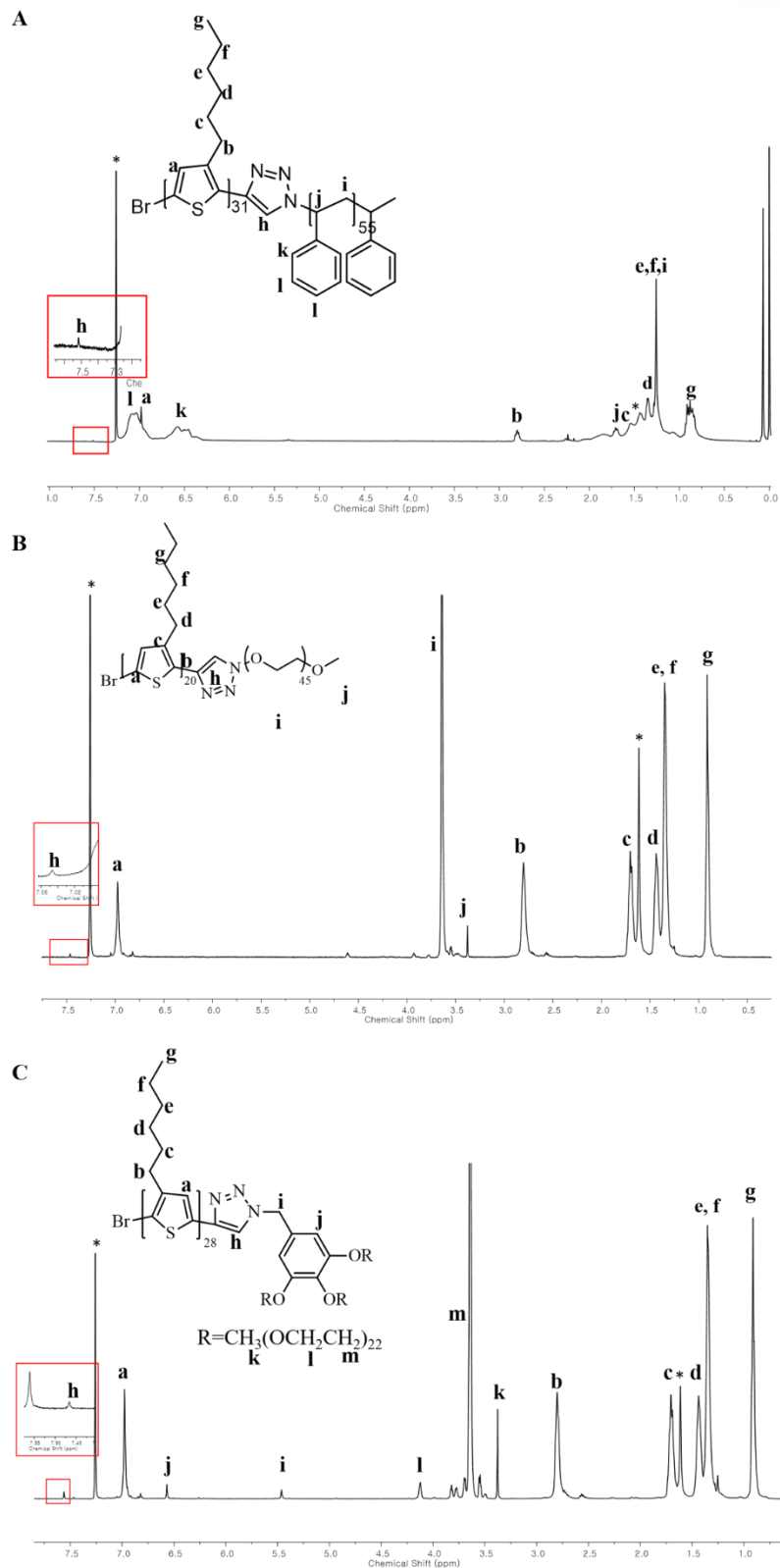
Figure 2.8 ^{1}H NMR spectra of π-conjugated block copolymer. (A) P3HT-*b*-PS. (B) P3HT-*b*-PEG2k. (C) P3HT-*b*-bPEG1k.

Solvent annealing of P3HT-*b*-PS

TEM images were obtained after solvent annealing for 3 hours. As shown in Figure 2.9, TEM images showed the nanofiber structure of P3HT-*b*-PS. When the annealing solvent used chloroform, the nanofibers were estimated to have a length of 600 ~ 700 nm (Figure 2.9A). When annealed with toluene, the nanofibers were similar in length to those with chloroform. (Figure 2.9B). These solvents are known as good solvents of P3HT. The good solvents did not significantly affected by the structure formed by solvent annealing of P3HT-*b*-PS thin films. The self-assembly behavior of rod-rod block copolymer was influenced by the various factors such as π-stacking and phase separation[25]. In the other conjugated block copolymer system, the nanofiber morphology has been seen and is typically driven by the packing of the conjugated block.
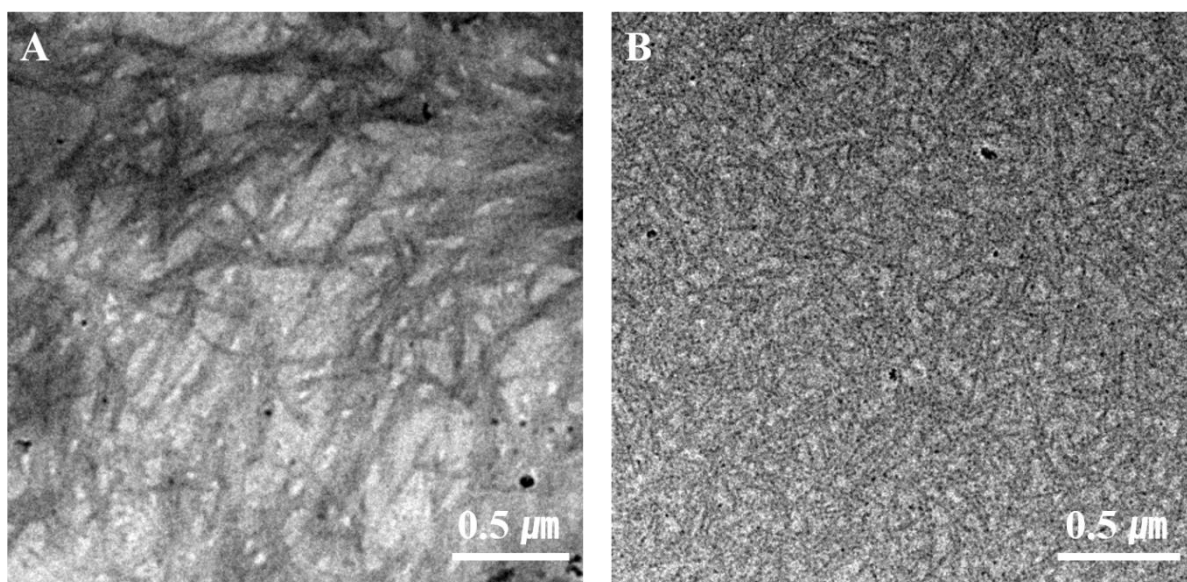
Figure 2.9 TEM images of nanofiber formed by different solvent annealing of P3HT-*b*-PS. Chloroform (A) and toluene (B).

Solution self-assembly of P3HT-*b*-PEG

We investigated the self-assembly behavior of P3HT-*b*-PEG in aqueous solution. Linear PEG (PEG2k) and branched PEG (bPEG1k) were used as a hydrophilic block. The block copolymer was dissolved in THF. Water was added to this solution at a controlled rate (0.5 mL/h) and stirred. The solution was dialyzed against water for 24 h to remove organic solvents. The self-assembled block copolymers were investigated by DLS, TEM, and AFM.

The diameter of block copolymers was measured by DLS. As shown in Figure 2.10, the average diameter of P3HT3.4k-*b*-PEG2k was estimated to be 508.5 nm and the average diameter of P3HT3.4k-*b*-bPEG1k was estimated to be 305.6 nm. Figure 2.11 shows the TEM images of nanofiber structure of P3HT-*b*-PEG. From the TEM image, the length of nanofibers increased with decreasing molecular weight of PEG when the P3HT block length was fixed. At bPEG1k and PEG2k, the length of nanofibers were 0.4 ~ 1.3 μm and 0.5 ~ 1.6 μm (Figure 2.11C-D), respectively. Similar behavior has been previously found in amphiphilic conjugated oligomers and can be explained by the reduction of the stretching energy of long PEG chanins through adopting shorter fibers[21]. As shown in Figure 2.11A and Figure 2.11C, the molecular weight of P3HT was increased by increasing the length of nanofiber when the molecular weight of PEG was fixed. The AFM image of P3HT3.4k-b-PEG2k appeared to have a thickness of 5.5 nm (Figure 2.12).
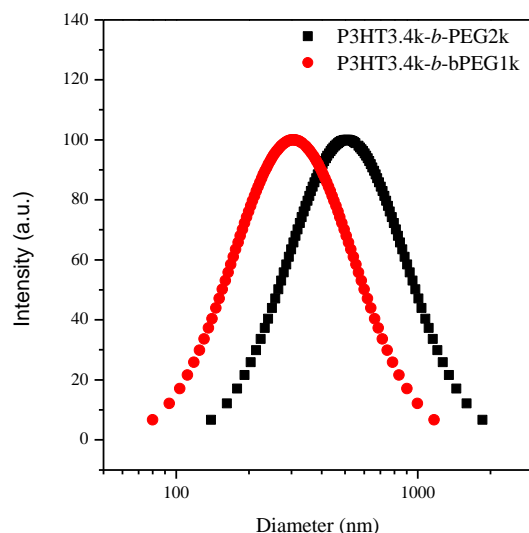
Figure 2.10 Size distribution of cylindrical micelles formed by self-assembly of P3HT-*b*-PEG.
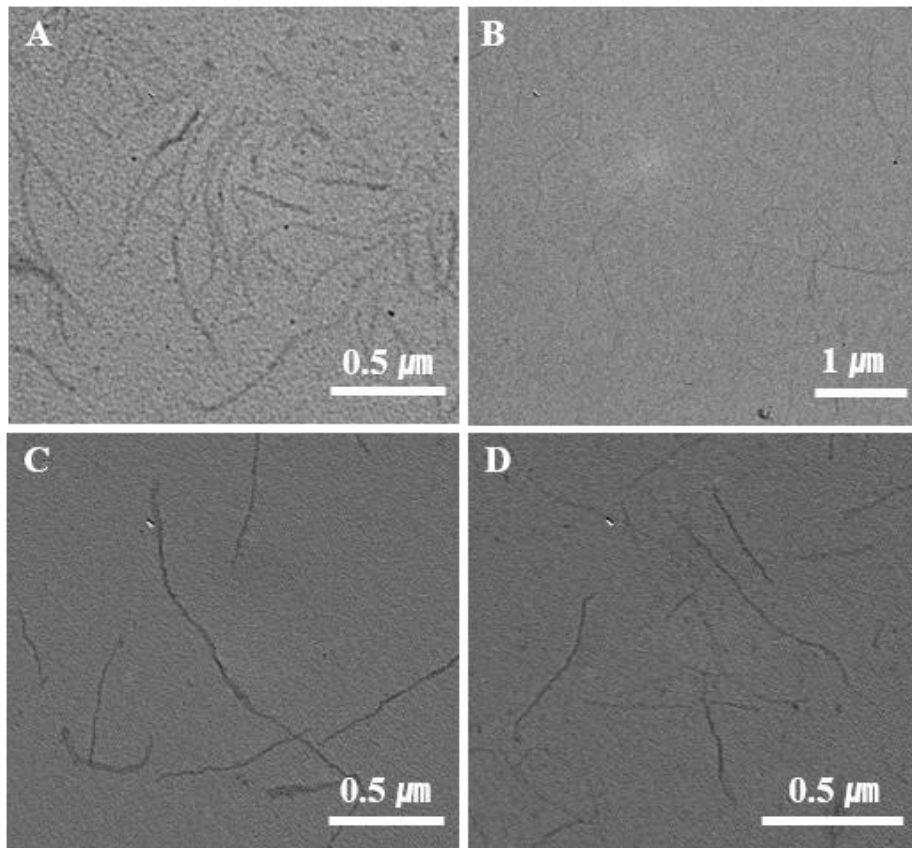
Figure 2.11 TEM images of cylindrical micelles formed by self-assembly of P3HT-*b*-PEG. (A) P3HT2.6k-*b*-PEG2k. (B) P3HT2.6k-*b*-bPEG1k. (C) P3HT3.4k-*b*-PEG2k. (D) P3HT3.4k-*b*-bPEG1k.
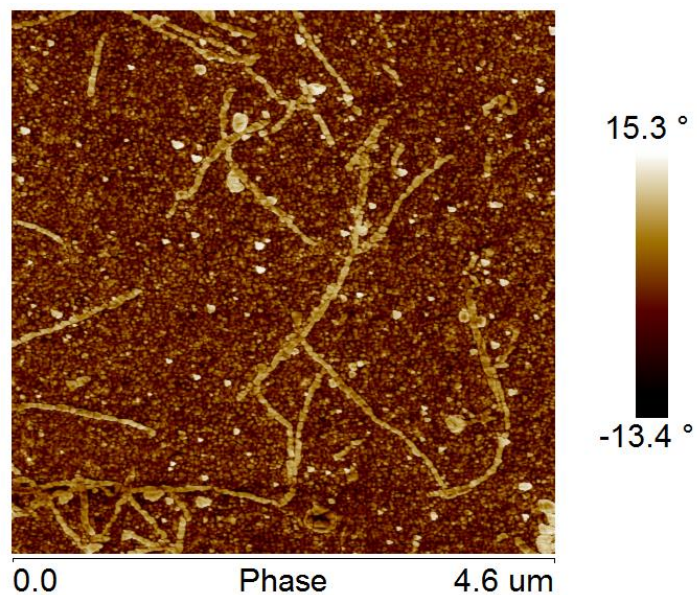
Figure 2.12 AFM image of cylindrical micelles formed by self-assembly of P3HT3.4k-*b*-PEG2k.

2.5 Summary

In summary, we synthesized ethynyl-terminated P3HT by the GRIM method in order to react with azide-terminated blocks. The molecular weight of P3HT measured by GPC was overestimated due to the rigid-rod conformation of P3HT. Conjugated block copolymer containing P3HT was synthesized by Cu(I)-catalyzed cycloaddition (click chemistry). The self-assembly behavior of the well-defined P3HT-*b*-PS in a thin film was studied by treating the thin films with solvent annealing using chloroform or toluene as a solvent. We found that the nanofiber structure formed by solvent annealing of P3HT-*b*-PS thin film was not significantly affected by solvent. The nanofiber morphology can be typically driven by the packing of the conjugated block. The self-assembly behavior of P3HT-*b*-PEG in aqueous solution was investigated. When the molecular weight of P3HT was fixed, the nanofiber increased with decreasing molecular weight of PEG due to the reduced stretching energy. This result showed that the nanofiber was not significantly influenced by the PEG block. The morphology of P3HT-containing block copolymer could be controlled by the molecular weight of PEG. The well-defined nanofiber is expected to be used in the fabrication of novel organic semiconducting nanostructures.

References

1. Xu, J.; Wang, J.; Mitchell, M.; Mukherjee, P.; Jeffries-El, M.; Petrich, J. W.; Lin, Z., Organic−Inorganic Nanocomposites via Directly Grafting Conjugated Polymers onto Quantum Dots. *J. Am. Chem. Soc.* **2007,** *129* (42), 12828-12833.

2. Lin, Z., Organic–Inorganic Nanohybrids through the Direct Tailoring of Semiconductor Nanocrystals with Conjugated Polymers. *Chem. Eur. J.* **2008,** *14* (21), 6294-6301.

3. Byun, M.; Laskowski, R. L.; He, M.; Qiu, F.; Jeffries-El, M.; Lin, Z., Controlled evaporative self-assembly of hierarchically structured regioregular conjugated polymers. *Soft Matter* **2009,** *5* (8), 1583-1586.

4. Javier, A. E.; Patel, S. N.; Hallinan, D. T.; Srinivasan, V.; Balsara, N. P., Simultaneous Electronic and Ionic Conduction in a Block Copolymer: Application in Lithium Battery Electrodes. *Angew. Chem., Int. Ed.* **2011,** *50* (42), 9848-9851.

5. Patel, S. N.; Javier, A. E.; Stone, G. M.; Mullin, S. A.; Balsara, N. P., Simultaneous Conduction of Electronic Charge and Lithium Ions in Block Copolymers. *ACS Nano* **2012,** *6* (2), 1589-1600.

6. Patel, S. N.; Javier, A. E.; Balsara, N. P., Electrochemically Oxidized Electronic and Ionic

Conducting Nanostructured Block Copolymers for Lithium Battery Electrodes. *ACS Nano* **2013,** *7* (7), 6056-6068.

7. Kline, R. J.; McGehee, M. D.; Kadnikova, E. N.; Liu, J.; Fréchet, J. M. J., Controlling the Field-Effect Mobility of Regioregular Polythiophene by Changing the Molecular Weight. *Adv. Mater.* **2003,** *15* (18), 1519-1522.

8. Joseph Kline, R.; McGehee, M. D.; Toney, M. F., Highly oriented crystals at the buried interface in polythiophene thin-film transistors. *Nat Mater* **2006,** *5* (3), 222-228.

9. Ballauff, M., Stiff-Chain Polymers—Structure, Phase Behavior, and Properties. *Angew. Chem., Int. Ed.* **1989,** *28* (3), 253-267.

10. McCullough, R. D.; Lowe, R. D., Enhanced electrical conductivity in regioselectively synthesized poly(3-alkylthiophenes). *J. Chem. Soc., Chem. Commun.* **1992,** (1), 70-72.

11. Chen, T.-A.; Wu, X.; Rieke, R. D., Regiocontrolled Synthesis of Poly(3-alkylthiophenes) Mediated by Rieke Zinc: Their Characterization and Solid-State Properties. *J. Am. Chem. Soc.* **1995,** *117* (1), 233-244.

12. Loewe, R. S.; Khersonsky, S. M.; McCullough, R. D., A Simple Method to Prepare Head-to-Tail Coupled, Regioregular Poly(3-alkylthiophenes) Using Grignard Metathesis. *Adv. Mater.* **1999,** *11* (3), 250-253.

13. Iovu, M. C.; Sheina, E. E.; Gil, R. R.; McCullough, R. D., Experimental Evidence for the Quasi-"Living" Nature of the Grignard Metathesis Method for the Synthesis of Regioregular Poly(3-alkylthiophenes). *Macromolecules* **2005,** *38* (21), 8649-8656.

14. Iovu, M. C.; Jeffries-El, M.; Zhang, R.; Kowalewski, T.; McCullough, R. D., Conducting Block Copolymer Nanowires Containing Regioregular Poly(3-Hexylthiophene) and Polystyrene. *J. Macromol. Sci., Part A: Pure Appl. Chem.* **2006,** *43* (12), 1991-2000.

15. Yen, W.-C.; Lee, Y.-H.; Lin, J.-F.; Dai, C.-A.; Jeng, U. S.; Su, W.-F., Effect of TiO2 Nanoparticles on Self-Assembly Behaviors and Optical and Photovoltaic Properties of the P3HT-b-P2VP Block Copolymer. *Langmuir* **2011,** *27* (1), 109-115.

16. He, M.; Zhao, L.; Wang, J.; Han, W.; Yang, Y.; Qiu, F.; Lin, Z., Self-Assembly of All-Conjugated Poly(3-alkylthiophene) Diblock Copolymer Nanostructures from Mixed Selective Solvents. *ACS Nano* **2010,** *4* (6), 3241-3247.

17. Wu, Z.-Q.; Ono, R. J.; Chen, Z.; Li, Z.; Bielawski, C. W., Polythiophene-block-poly([gamma]-benzyl L-glutamate): synthesis and study of a new rod-rod block copolymer. *Polym. Chem.* **2011,** *2* (2), 300-302.

18. Lee, E.; Hammer, B.; Kim, J.-K.; Page, Z.; Emrick, T.; Hayward, R. C., Hierarchical Helical Assembly of Conjugated Poly(3-hexylthiophene)-block-poly(3-triethylene glycol thiophene) Diblock Copolymers. *J. Am. Chem. Soc.* **2011,** *133* (27), 10390-10393.

19. Patra, S. K.; Ahmed, R.; Whittell, G. R.; Lunn, D. J.; Dunphy, E. L.; Winnik, M. A.; Manners, I., Cylindrical Micelles of Controlled Length with a π-Conjugated Polythiophene Core via Crystallization-Driven Self-Assembly. *J. Am. Chem. Soc.* **2011,** *133* (23), 8842-8845.

20. Yu, W.; Yang, D.; Zhu, X.; Wang, X.; Tu, G.; Fan, D.; Zhang, J.; Li, C., Control of Nanomorphology in All-Polymer Solar Cells via Assembling Nanoaggregation in a Mixed Solution. *ACS Appl. Mater. Interfaces* **2014,** *6* (4), 2350-2355.

21. Kamps, A. C.; Fryd, M.; Park, S.-J., Hierarchical Self-Assembly of Amphiphilic Semiconducting Polymers into Isolated, Bundled, and Branched Nanofibers. *ACS Nano* **2012,** *6* (3), 2844-2852.

22. Wu, P.-T.; Ren, G.; Li, C.; Mezzenga, R.; Jenekhe, S. A., Crystalline Diblock Conjugated Copolymers: Synthesis, Self-Assembly, and Microphase Separation of Poly(3-butylthiophene)-b-poly(3-octylthiophene). *Macromolecules* **2009,** *42* (7), 2317-2320.

23. Hammer, B. A. G.; Bokel, F. A.; Hayward, R. C.; Emrick, T., Cross-Linked Conjugated Polymer Fibrils: Robust Nanowires from Functional Polythiophene Diblock Copolymers. *Chem. Mater.* **2011,** *23* (18), 4250-4256.

24. Kim, K. T.; Vandermeulen, G. W. M.; Winnik, M. A.; Manners, I., Organometallic−Polypeptide Block Copolymers: Synthesis and Properties of Poly(ferrocenyldimethylsilane)-b-poly- (γ-benzyl-l-glutamate). *Macromolecules* **2005,** *38* (12), 4958-4961.

25. Liu, J.; Sheina, E.; Kowalewski, T.; McCullough, R. D., Tuning the Electrical Conductivity and Self-Assembly of Regioregular Polythiophene by Block Copolymerization: Nanowire Morphologies in New Di- and Triblock Copolymers. *Angew. Chem., Int. Ed.* **2002,** *41* (2), 329-332.

3. Synthesis of bent-core liquid crystals

3.1 Abstract

The well-defined structure of bent-core liquid crystals has physicochemical properties. We synthesized two chiral bent-core mesogens $Pn-O-PIMB(n-2)*$ ($n = 8$ and 9) and a achiral bent-core mesogen P8-O-PIMB in order to observe the morphology of bent-core mesogens in the 60 nm AAO nanochannel. These bent-core mesogens were confirmed by NMR and EI-mass. The phase transition temperature of bent-core mesogens measured by DSC was comparable to previous reports. The morphologies of bent-core liquid crystals in the 60 nm AAO nanochannel were studied by depolarized reflected light microscopy (DRLM), scanning electron microscopy (SEM), and grazing incidence X-ray diffraction (GIXD).

3.2 Introduction

The field of liquid crystals has been an active and fruitful research area for many years. There are many applications of liquid crystals such as displays[1-3], sensors[4-6], and fibres[7-8]. Niori et al. discovered that achiral bent-core (banana shaped) molecules possess unusual and interesting properties such as unique polarity and supramolecular chirality[9]. The investigation of the relationship between the molecular structure and mesomorphic properties is very important to liquid crystal chemistry. These new mesophases are classified from B_1 to B_7 phases depending on packing arrangement[10-14]. The well-defined structures of bent-core mesogens have exotic physicochemical properties[15-16]. The properties originate from spontaneously broken symmetries even though the LC material itself does not have any chiral centre such as a chiral carbon. A strong nanosegregation of bent-core molecules can result in macroscopic polar, chiral, or in some cases, modulated layered structures, forming a variety of ferroelectric or anti-ferroelectric phases that are useful for opto-electronic applications such as non-linear optics[17-18].

Clark and co-workers reported the helical structure of smectic liquid crystal[19]. Walba and co-workers reported spontaneous formation of macroscopic chiral domains in a fluid smectic phase of achiral molecules[20]. Takezoe and co-workers reported a racemic layer structure in a chiral bent-core ferroelectric liquid crystal[21]. Yoon et al. reported Physico-chemical confinement of helical nanofilaments using bent-core mesogens and a twist-grain-boundary structure in the B4 phase of a bent-core molecular system identified by second harmonic generation circular dichroism measurement[22].

In this study, we synthesized bent-core mesogens inducing spontaneous chirality in order to obtain well-defined morphology in the 60 nm AAO nanochannel. The bent-core mesogens were characterized

by NMR and EI mass spectroscopy. The phase transition temperature of bent-core mesogenes was measured by DSC. The morphologies of bent-core liquid crystals in 60 nm AAO nanochannel was studied by depolarized reflected light microscopy (DRLM), scanning electron microscopy (SEM), and grazing incidence X-ray diffraction (GIXD).

3.3 Experimental

Materials and Methods

Differential scanning calorimetry (DSC) was performed using a Mettler-Toledo DSC823e under an atmosphere of nitrogen at a heating/cooling rate of 5 °C/min.

Optical anisotropy measurements using cross polarizers were performed by depolarized reflected light microscopy (DRLM, Nikon LV100POL).

GIXD experiments were carried out at PLS-II (Pohang Accelerator Laboratory) in the Republic of Korea. The samples were prepared with the same dimensions of 10 mm x 10 mm (in-plane area) x 180 μm (depth). The incidence X-ray beam was guided to the samples with an energy of 11.15 keV, a size of 70 μm (vertical) x 300 μm (horizontal) and a sample-to-detector distance (SDD) of 235 mm. To investigate the in situ molecular orientation sequences, molecular cooling was conducted with a precisely controlled temperature gradient from 165 °C to 25 °C at a cooling rate of 5 °C/min. All diffraction patterns were acquired at every phase transition after 5 min of dwelling time to reach the thermal equilibrium state in each case. Before and after all GIXD experiments, morphological measurements were conducted to confirm the variations in LC structure under different surface conditions.
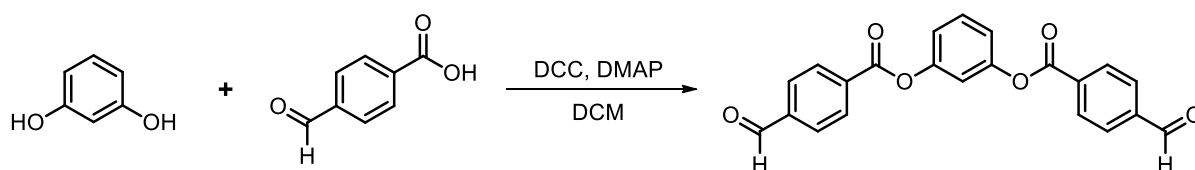
Scheme 3.1 Synthesis of 1,3-phenylene bis(4-formylbenzoate).

Synthesis of 1,3-phenylene bis(4-formylbenzoate)

1,3-Dicyclohexylcarbodiimide (DCC) (37.48 g, 181.64 mmol) was dissolved in dry DCM and then a

solution of resorcinol (5 g, 45.41 mmol) and 4-formylbenzoic acid (20.45 g, 136.23 mmol) in dry THF was added. Finally 4-(N,N-dimethylamino)pyridine (DMAP) (3.16 g, 25.88 mmol) was added. The mixture was stirred at room temperature under nitrogen overnight. The mixture was filtrated on silica gel column chromatography (DCM) and recrystallized from THF and DCM. ^{1}H NMR (CDCl$_3$, ppm): δ 10.15 (s, 2H), 8.37 (m, 4H), 8.04 (m, 4H), 7.53 (t, J = 8.2 Hz, 1H), 7.25 (t, J = 2.2 Hz, 1H), 7.22 (dd, J = 8.2 Hz, 2.2 Hz, 2H).
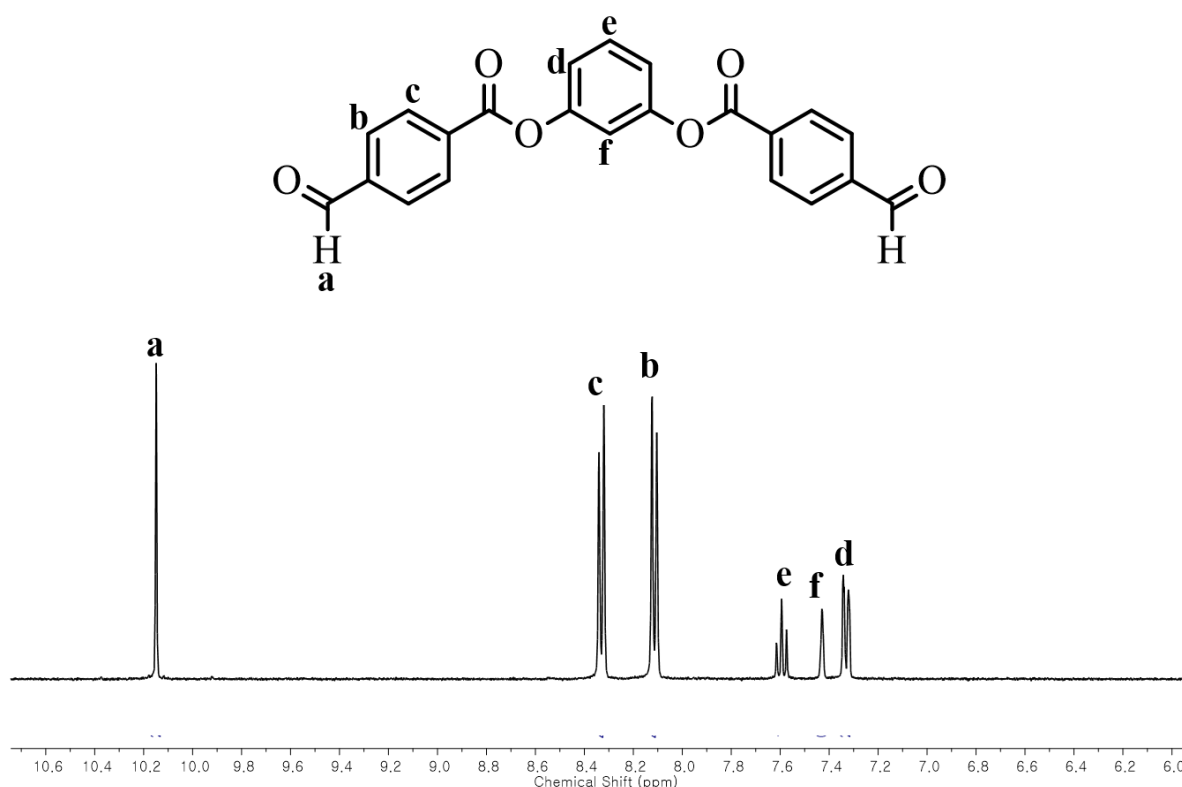
**Figure 3.1** ^{1}H NMR spectra of 1,3-phenylene bis(4-formylbenzoate).
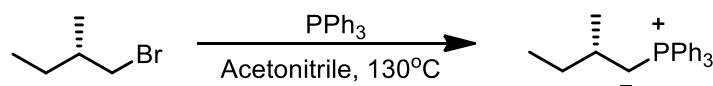
Scheme 3.2 Synthesis of phosphonium salt.

Synthesis of phosphonium salt

An acetonitrile solution of (*S*)-(+)-1-bromo-2-methylbutane (10 g, 66.20 mmol) and triphenylphosphine (14.47 g, 55.17 mmol) was stirred at 130 °C for 3 days. The solvent was evaporated and residue was washed with hexane several times by decantation to remove any unreacted

triphenylphosphine. The crude phosphonium salt was dried in vacuo at 80 °C overnight. ^{1}H NMR (CDCl$_3$, ppm): δ 7.90-7.67 (m, 15H), 3.81-3.57 (m, 2H), 1.86-1.72 (m, 1H), 1.53-1.39 (m, 2H), 0.96 (d, J = 6.7 Hz, 3H), 0.8 (t, J – 7.4 Hz, 3H).
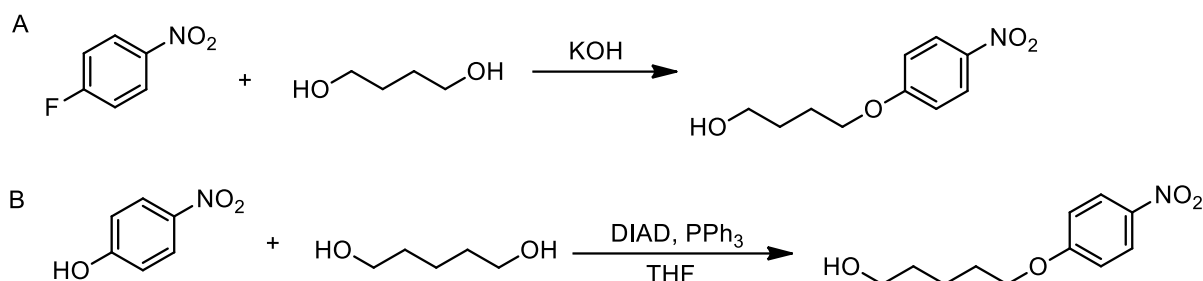
Scheme 3.3 Synthesis of alcohols.

Synthesis of 4-(4-nitrophenoxy)butan-1-ol (1a)

To mixture of 1,4-butanediol (31.9 g, 354 mmol) and potassium hydroxide (5 g, 89.1 mmol) was slowly added dropwise *p*-nitrofluorobenzene (10 g, 70.7 mmol) at room temperature overnight. The reaction mixture was then poured into water and extracted with DCM. Finally the mixture was washed with brine. The combine organic extract was dried by MgSO$_4$, then concentrated to a crude product. The crude product was recrystallized from ethyl acetate and hexane several times to give the product as a white solid. ^{1}H NMR (CDCl$_3$, ppm): δ 8.19 (d, J = 9.2 Hz, 2H), 6.94 (d, J = 9.2 Hz, 2H), 4.06 (t, J = 6.3 Hz, 2H), 3.78-3.71 (m, 2H), 1.98-1.90 (m, 2H), 1.81-1.72 (m, 2H), 1.43 (t, J = 5.2 Hz, 1H).

Synthesis of 5-(4-nitrophenoxy)pentan-1-ol (1b)

To a dry THF solution of p-nitrophenol (2.08 g, 15.0 mmol), tripheylphosphine (5.11 g, 19.5 mmol), and 1,5-pentanediol (4.69 g, 45.0 mmol) at 0 °C was added diisopropylazodicarboxylate (DIAD, 3.94 g, 19.5 mmol). The mixture was allowed to warm up to room temperature and stirred overnight. The solvent was concentrated on a rotary evaporator. This mixture was extracted with ether and 1 M NaOH and then washed with brine. The organic layer was dried with MgSO$_4$, concentrated. The mixture was purified by silica column chromatography (EA/Hx = 3/1, v/v). ^{1}H NMR (CDCl$_3$, ppm): δ 8.19 (d, J = 9.3 Hz, 2H), 6.94 (d, J = 9.3 Hz, 2H), 4.06 (t, J = 6.4 Hz, 2H), 3.69 (t, J = 6.3 Hz, 2H), 1.90-1.82 (m, 2H), 1.72-1.52 (m, 6H).

Synthesis of aldehyde (2)

2a To a solution of fragment distilled oxalyl chloride (3.61 g, 28.43 mmol) in dry DCM at -78 °C was added dropwise a solution of dry dimetylsulfoxide (DMSO) (3.00 g, 38.37 mmol) in dry DCM. After

being stirred for 2 hours under nitrogen, 4-(4-nitrophenoxy)pentan-1-ol (3.00 g, 14.21 mmol) in dry DCM was added and the mixture was stirred for 3 hours. Dry triethylamine (TEA) (14.38 g, 142.13 mmol) was added to the solution and the mixture was stirred for 2 hours. The reaction mixture was allowed to warm up to room temperature and quenched by adding saturated aqueous ammonium chloride solution. The mixture was extracted with DCM. The combined organic extract was washed with brine, dried by $MgSO_4$, and concentrated. The mixture was purified by silica gel column chromatography (DCM/Hx = 2/1, v/v) to give 4-(4-nitrophenoxy)butanal. ^{1}H NMR ($CDCl_3$, ppm): δ 9.85 (t, J = 1.1 Hz, 1H), 8.20 (d, J = 9.2 Hz, 2H), 6.94 (d, J = 9.3 Hz, 2H), 4.10 (t, J = 6.1 Hz, 2H), 2.70 (td, J = 6.9 Hz, 1.1 Hz, 2H), 2.21-2.13 (m, 2H).

2b 5-(4-nitrophenoxy)pentanal was prepared similarly to the 5-(4-nitrophenoxy)pentan-1-ol. ^{1}H NMR ($CDCl_3$, ppm): δ 9.81 (t, J = 1.4 Hz, 1H), 8.20 (d, J = 9.2 Hz, 2H), 6.94 (d, J = 9.3 Hz, 2H), 4.07 (t, J = 5.9 Hz, 2H), 2.56 (td, J = 6.9 Hz, 1.4 Hz, 2H), 1.90-1.82 (m, 4H).

Synthesis of p-alkoxyanilines (4)

4a To a suspension of phophonium salt (7.80 g, 17.22 mmol) in dry THF at -78 °C was added n-BuLi (1.6 M hexane solution, 9.57 ml, 15.31 mmol). The mixture was stirred for 1 h, and 4-(4-nitro phenoxy) butanal (2 g, 9.57 mmol) in dry THF was added. The solution was stirred overnight at room temperature and the reaction was quenched with saturated aqueous NH_4Cl solution. The solvent was removed with a rotary evaporator. This mixture was extracted with hexane and washed with brine. The combined organic extract was dried by $MgSO_4$, then concentrated. The mixture was purified by silica gel column chromatography (EA/Hx = 1/49, v/v). An ethanol solution of (S)-1-((6-methylnon-4-en-1-yl)oxy)-4-nitrobenzene (1 g, 3.8 mmol) was treated with palladium on charcoal (5%, 0.4 mg, 3.8 mmol) at room temperature overnight under hydrogen bubbling and the reaction was finished after removal of the vinyl group was confirmed by ^{1}H NMR trace. The reaction mixture was filtered with the aid of based alumina oxide in chloroform. The filtered solution was concentrated and purified by silica gel column chromatography (EA/Hx = 1/1, v/v) to give (S)-4-((6-methylnonyl)-oxy)aniline. ^{1}H NMR ($CDCl_3$, ppm): δ 6.74 (d, J = 8.6 Hz, 2H), 6.64 (d, J = 8.3 Hz, 2H), 3.88 (t, J = 6.6 Hz, 2H), 3.40 (br s, 1H), 1.79-1.70 (m, 2H), 1.46-1.26 (m, 9 H), 1.19-1.07 (m, 2H), 0.86 (t, J = 7.0 Hz, 6H).

4b In essentially the same manner Synthesis (S)-5-((7-methylnonyl)oxy)aniline was prepared. ^{1}H NMR ($CDCl_3$, ppm): δ 6.74 (d, J = 9.0 Hz, 2H), 6.63 (d, J = 9.0 Hz, 2H), 3.87 (t, J = 6.6 Hz, 2H), 3.4 (br s, 1H), 1.73 (m, 2H), 1.48-1.05 (m, 13 H), 0.89-0.82 (m, 6H).

Synthesis of Pn-O-PIMB(n-2)* (5)

5a A solution of 1,3-Phenylenebis(4-formyl-benzoate) (0.072 g, 0.19 mmol) and (S)-4-((6-methylnonyl)-oxy)aniline (0.1 g, 0.43 mmol) in chloroform was refluxed for 1 day. The reaction mixture was concentrated, washed with ethanol and recrystallized with chloroform and ethanol to give P8-O-PIMB6*. ^{1}H NMR (CDCl$_3$, ppm): δ 8.58 (s, 2H), 8.29 (d, J = 8.3 Hz, 4H), 8.03 (d, J = 8.4 Hz, 4H), 7.51 (t, J = 8.2 Hz, 1H), 7.33-7.19 (m, 7H), 3.99 (t, J = 6.6 Hz, 4H), 1.87-1.76 (m. 4H), 1.51-1.07 (m, 18H), 0.87 (t, J = 6.3 Hz, 12H) , ^{13}C NMR (CDCl$_3$, ppm): δ 164.33, 158.49, 156.22, 151.39, 143.88, 141.11, 130.92, 130.55, 129.91, 128.51, 122.44, 119.27, 115.75, 115.04, 68.31, 36.50, 34.34, 29.47, 29.31, 26.86, 26.38, 19.20, 11.39. MS (EI) calcd. for C$_{52}$H$_{60}$N$_2$O$_6$ 808.45, found 808.

5b Similarly, the reaction of 1,3-Phenylenebis(4-formyl-benzoate) and (S)-5-((7-methylnonyl)oxy) aniline) gave P9-O-PIMB7* as a yellow crystal. ^{1}H NMR (CDCl$_3$, ppm): δ 8.58 (s, 2H), 8.28 (d, J = 8.2 Hz, 4H), 8.03 (d, J = 8.2 Hz, 4H), 7.51 (t, J = 8.0 Hz, 1H), 7.34-7.18 (m, 7H), 6.95 (d, J = 8.7 Hz, 4H), 3.99 (t, J = 6.5 Hz, 4H), 1.80 (quin, J = 6.6 Hz, 4H), 1.54-1.05 (m, 22H), 0.94-0.76 (m, 12H), ^{13}C NMR (CDCl$_3$, ppm): δ 164.36, 158.52, 156.24, 151.41, 143.89, 141.13, 130.93, 130.57, 129.93, 128.53, 122.46, 119.29, 115.77, 115.05, 68.31, 36.54, 34.38, 29.75, 29.48, 29.29, 27.00, 26.07, 19,22, 11.40. MS (EI) calcd. for C$_{54}$H$_{64}$N$_2$O$_6$ 836.48, found 836.

Synthesis of N-(4-(octyloxy)phenyl) acetamide (6)

A mixture of 4-acetamidophenol (15 g, 99.23 mmol) and 1-bromooctane (21.05 g, 109.00 mmol) in acetone was stirred and then potassium carbonate (45.20 g, 327.00 mmol) was slowly added. The mixture was refluxed overnight. The solvent was removed with a rotary evaporator. This mixture was purified by recrystallization from ethanol three times. ^{1}H NMR (CDCl$_3$, ppm): δ 7.36 (d, J = 9.0 Hz, 2H), 7.04 (s, 1H), 6.84 (d, J = 8.9 Hz, 2H), 3.92 (t, J = 6.6 Hz, 2H), 2.15 (s, 3H), 1.80-1.71 (m, 2H), 1.50-1.23 (m, 10H).

Synthesis of 4-(Octyloxy)aniline (7)

To an ethanol solution of N-(4-(octyloxy)phenyl) acetamide (20 g, 75.94 mmol) was added HCl solution (10 v/v%) and stirred overnight at 70 ℃. The solvent was removed with a rotary evaporator. This mixture was extracted with ether and water three times. Finally the mixture was washed with brine. The combined organic extract was dried by MgSO$_4$, concentrated. The mixture was purified by silica gel column chromatography (EA/Hx=1/1, v/v). ^{1}H NMR (CDCl$_3$, ppm): δ 6.74 (d, J = 8.9 Hz, 2H), 6.63

(d, J = 8.9 Hz, 2H), 3.89 (t, J = 6.6 Hz, 2H), 3.40 (s, 2H), 1.78-1.69 (m, 2H), 1.48-1.22 (m, 10H), 0.88 (t, J = 6.8 Hz, 3H).

Synthesis of P8-O-PIMB6 (8)

A solution of 4-(Octyloxy)aniline (2.13 g, 9.62 mmol) and 1,3-Phenylene bis(4-formyl-benzoate) (1.5 g, 4.01 mmol) in chloroform was refluxed overnight. The mixture was concentrated on a rotary evaporator and recrystallized with chloroform and ethanol to give P8-O-PIMB6. ^{1}H NMR (CDCl$_3$, ppm): δ.58 (s, 2H), 8.28 (d, J = 8.3Hz, 4H), 8.03 (d, J = 8.3Hz, 4H), 7.51 (t, J = 8.2Hz, 1H), 7.29 (d, J = 9.0Hz, 4H), 7.19-7.25 (m, 3H), 6.95 (d, J = 9.0Hz, 4H), 3.99 (t, J = 6.6 Hz, 4H), 1.84-1.76 (m, 4H), 1.52-1.25 (m, 20H), 0.894 (t, J = 7.2Hz, 6H). ^{13}C NMR (CDCl$_3$, ppm): δ 164.34, 158.49, 156.22, 151.39, 143.88, 141.11, 130.91, 130.55, 129.91, 128.51, 122.43, 119.27, 115.75, 115.04, 68.31, 31.80, 29.35, 29.27, 29.22, 26.04, 22.64, 14.08. MS (EI) calcd. for C$_{50}$H$_{56}$N$_2$O$_6$ 780.99, found 781

Optical texture analysis in bulk state

The phase transition behaviors of the bent-core liquid crystals on the glass substrate were controlled by the cooling rate 1 °C/min.

### Morphology analysis of bent-core liquid crystal in 60 nm AAO nanochannel

To chemically modify the walls of the AAO nanochannels effectively, silica coating via a sol–gel method was necessary. Dried AAO was immersed in a SiCl$_4$ precursor and then rinsed with hexane, methanol, and ethanol. After drying in nitrogen gas, the AAO was heated to 120 °C over 1 h; this process was repeated three times. With this step, the inner wall of AAO and the surface of the silicon wafer contain the same surface component (SiO$_2$) that is guaranteed to be identical for further surface modification. Each surface feature (silanol-terminated AAO and SiO$_2$-containing silicon wafer) was chemically modified with OTS (Gelest) and PEG 6/9 (90%, Gelest) as self-assembled monolayers. Bent-core LCs were simply loaded into the nanochannels by capillary force at the isotropic temperature.

3.4 Results and Discussion
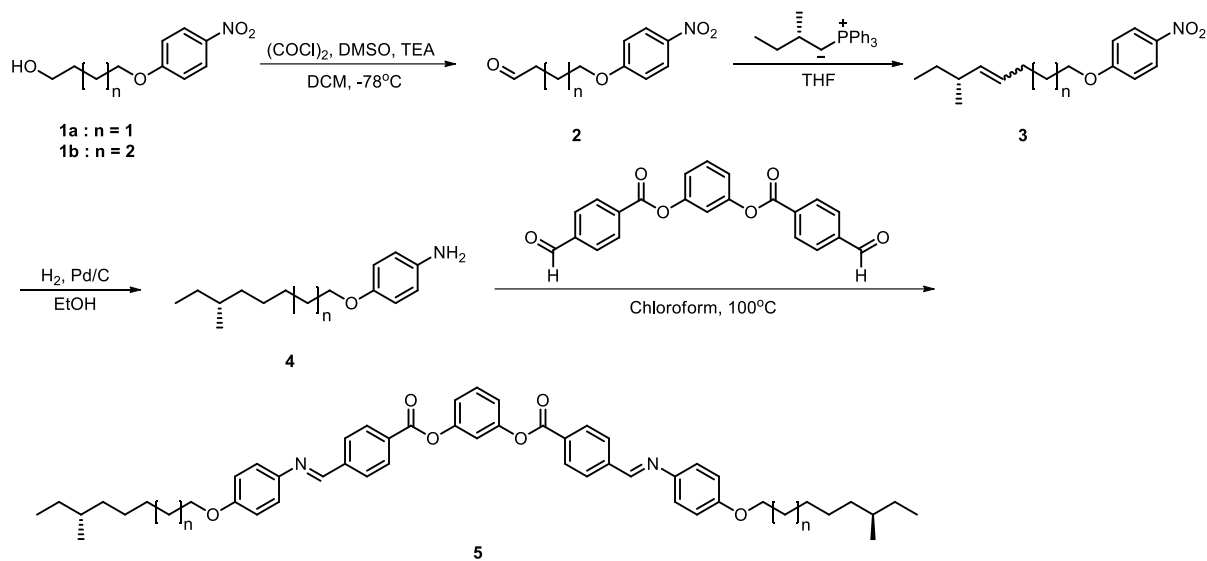
Scheme 3.4 Synthesis of Pn-O-PIMB(n-2)*.

We synthesized banana-shaped (bent-core) chiral LC molecules as shown in Scheme 3.4. The general structure of bent-core LC was confirmed by ^{1}H NMR and ^{13}C NMR (Figure 3.2 and Figure 3.3).
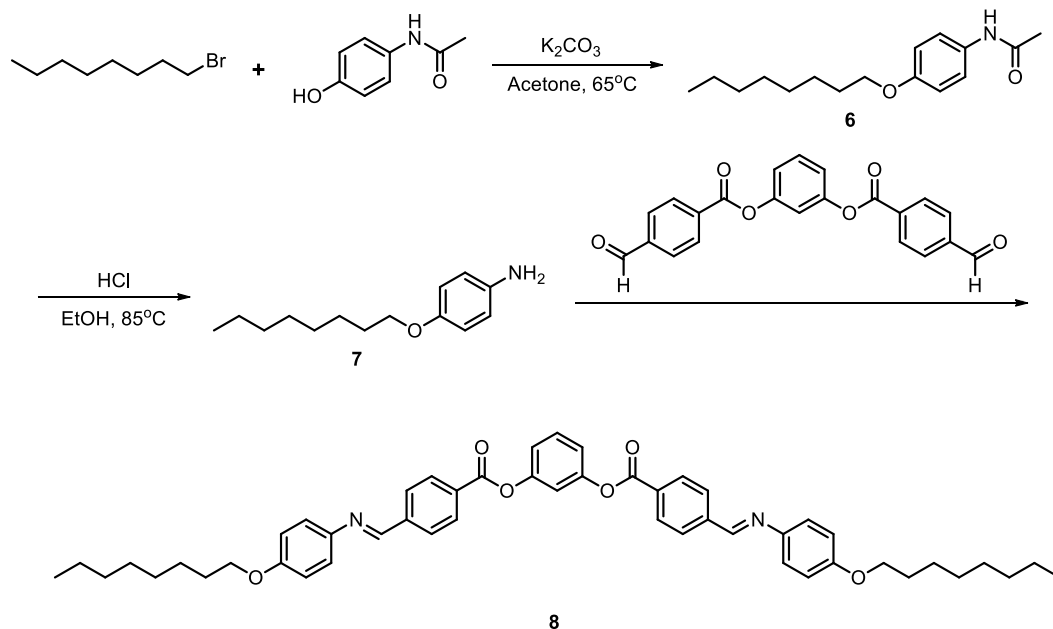
Scheme 3.5 Synthesis of P8-O-PIMB6.

Also, we synthesized achiral bent-core LC molecules as shown in Scheme 3.5. This molecular structure was confirmed by ^{1}H NMR and ^{13}C NMR (Figure 3.4).

A

B
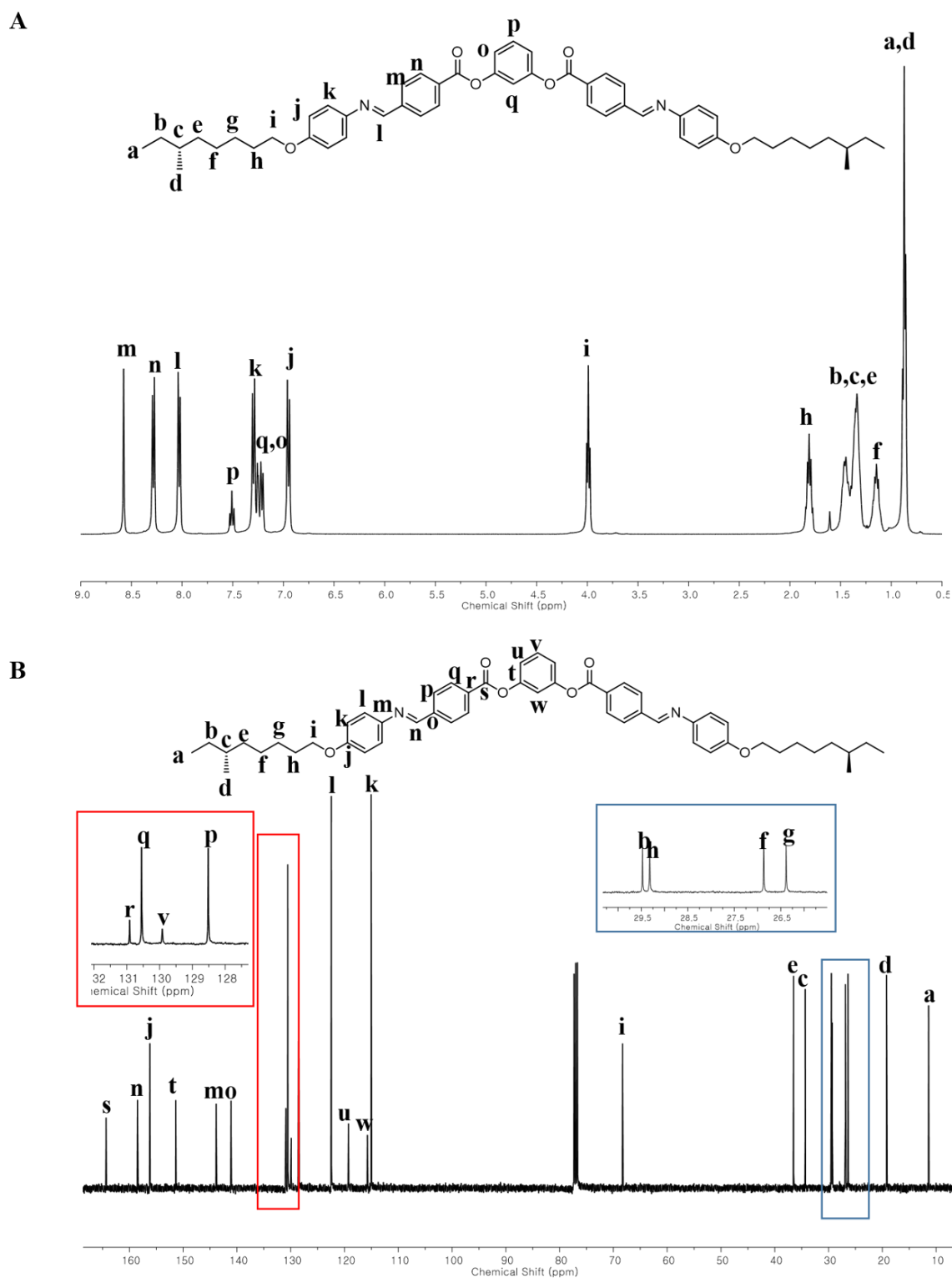

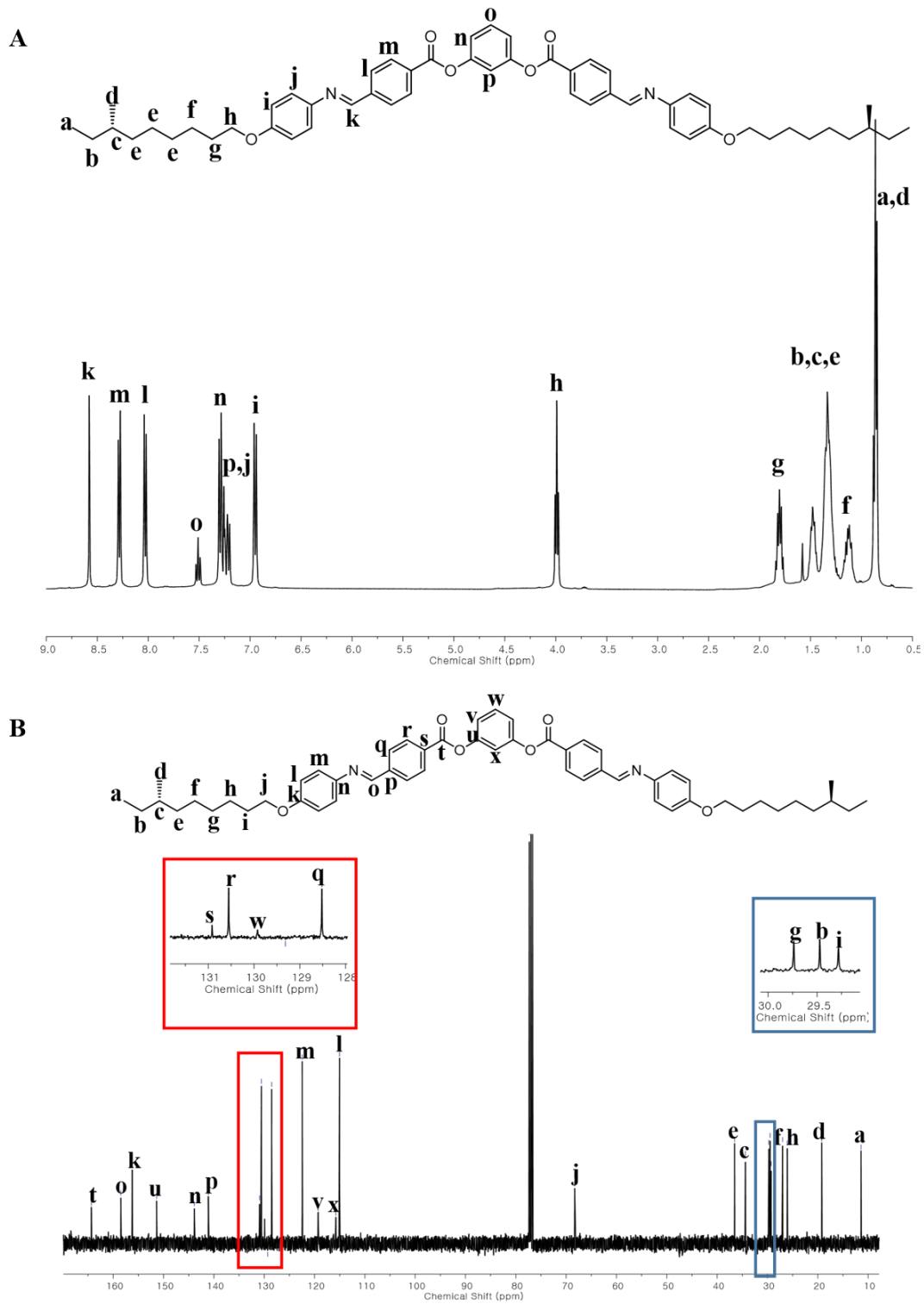**Figure 3.2** NMR spectra of P8-O-PIMB6*. ^{1}H NMR (A) and ^{13}C NMR (B).

4 2

A

B

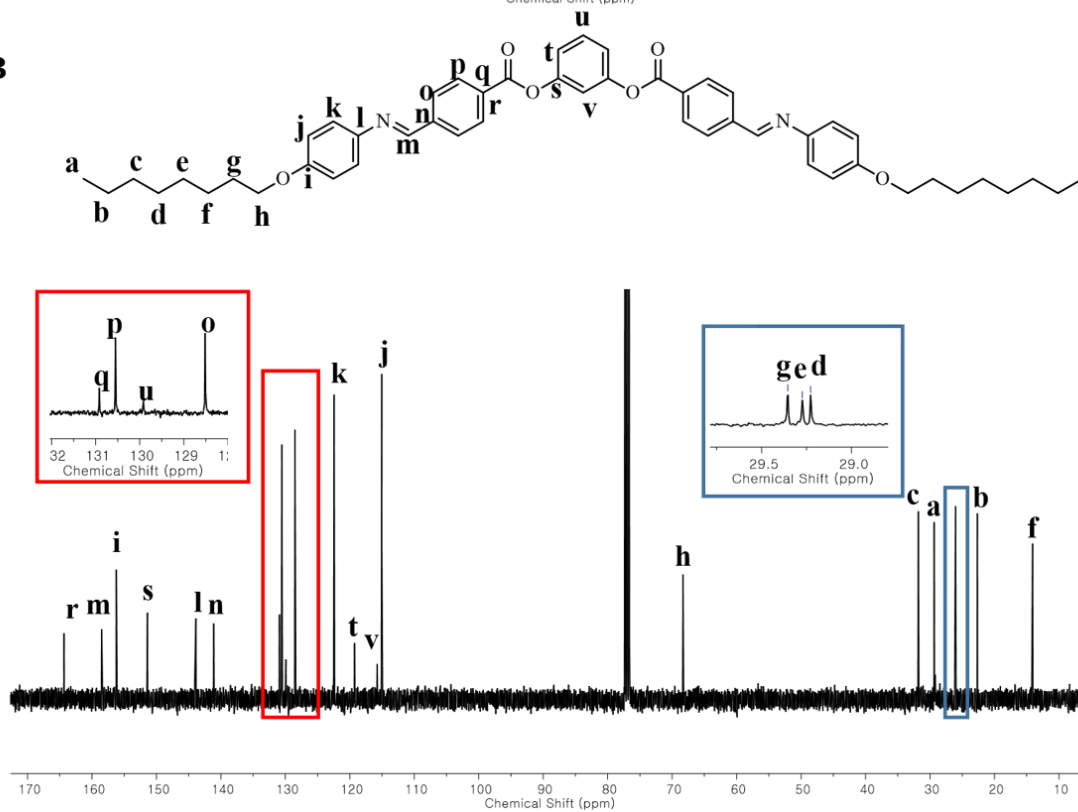**Figure 3.3** NMR spectra of P9-O-PIMB7*. ^{1}H NMR (A) and ^{13}C NMR (B).

Figure 3.4 NMR spectra of P8-O-PIMB6. ^{1}H NMR (A) and ^{13}C NMR (B).

The transition temperature of bent-core LC was measured by DSC as shown in Figure 3.5. P8-O-PIMB6 was exhibited 158 ℃ and 175 ℃ in the heating cycle and 141 ℃, 148 ℃ and 173 ℃ in the cooling cycle (Figure 3.4A). P8-O-PIMB6 was exhibited 148 ℃ and 170 ℃ in the heating cycle and 132 ℃ and 162 ℃ in the cooling cycle (Figure 3.4B). These transition temperatures of bent-core mesogens were comparable to the previous report[23]. P8-O-PIMB6* and P8-O-PIMB6 are expected to observe the structures in these three states as being $SmC_AP^*_F$, $SmC_SP^*_F$ and $SmC_SP^*_A$ according to temperature and could provide well-defined morphology under an electric field.
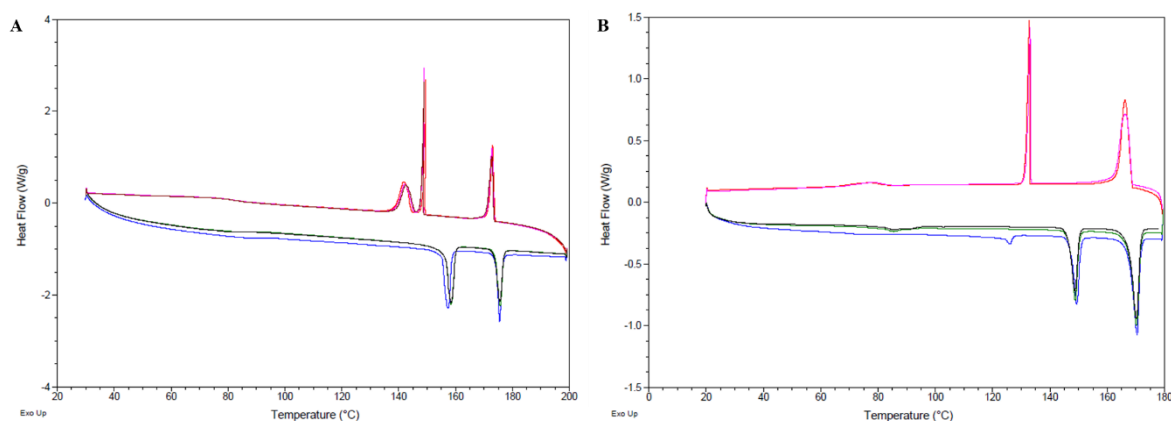

Figure 3.5 Transition temperature graph measured by DSC. P8-O-PIMB6 (A) and P8-O-PIMB6* (B).

Morphologies of bent-core liquid crystals in 60 nm AAO channel

Optical textures of P8-O-PIMB6* and P9-O-PIMB7* were observed, as shown in Figure 3.6. The bent-core mesogens were expected to exhibit a phase transition to B_4-like texture (helical layer)[21]. The morphology of P8-O-PIMB6* (Figure 3.6A) exhibited B_2-like texture at 165 ℃, but did not show B_4-like texture at 140 ℃. The morphology of P9-O-PIMB7* (Figure 3.6B) also showed a similar phase transition; B_2-like texture was exhibited at 167 ℃, but B_4-like texture was not exhibited. By observing the morphology of the bent-core liquid crystal in the 60 nm AAO nanochannel on SEM and GIXD, we identified cylindrical structure (Figure 3.7). The result implies additional chiral carbon irritates symmetry-broken molecular packing due to steric hindrance. Therefore, the morphology of bent-core liquid crystal could not phase transition to helical structure.
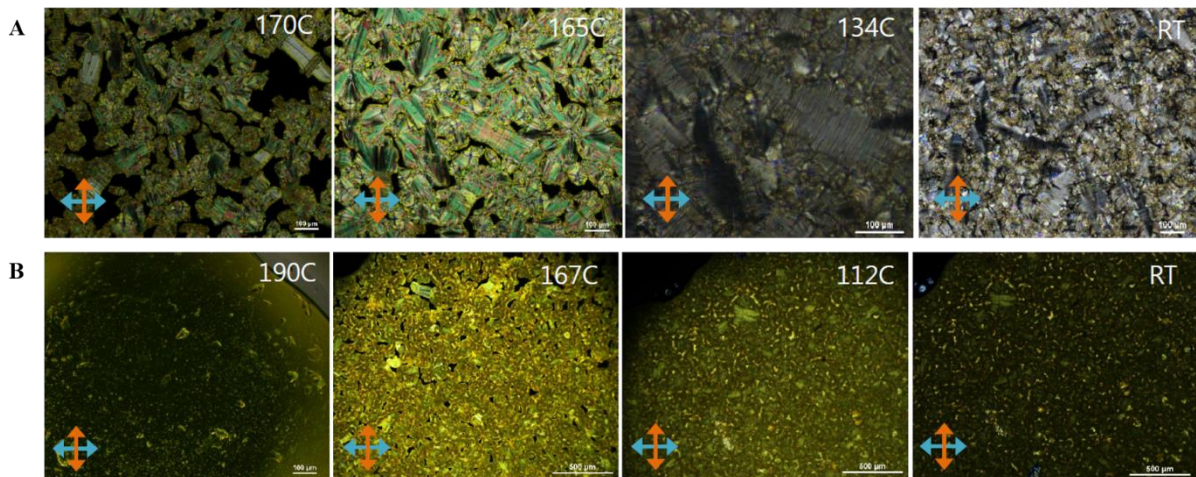
Figure 3.6 Optical texture of bent-core liquid crystals. (A) P8-O-PIMB6*. (B) P9-O-PIMB7*.
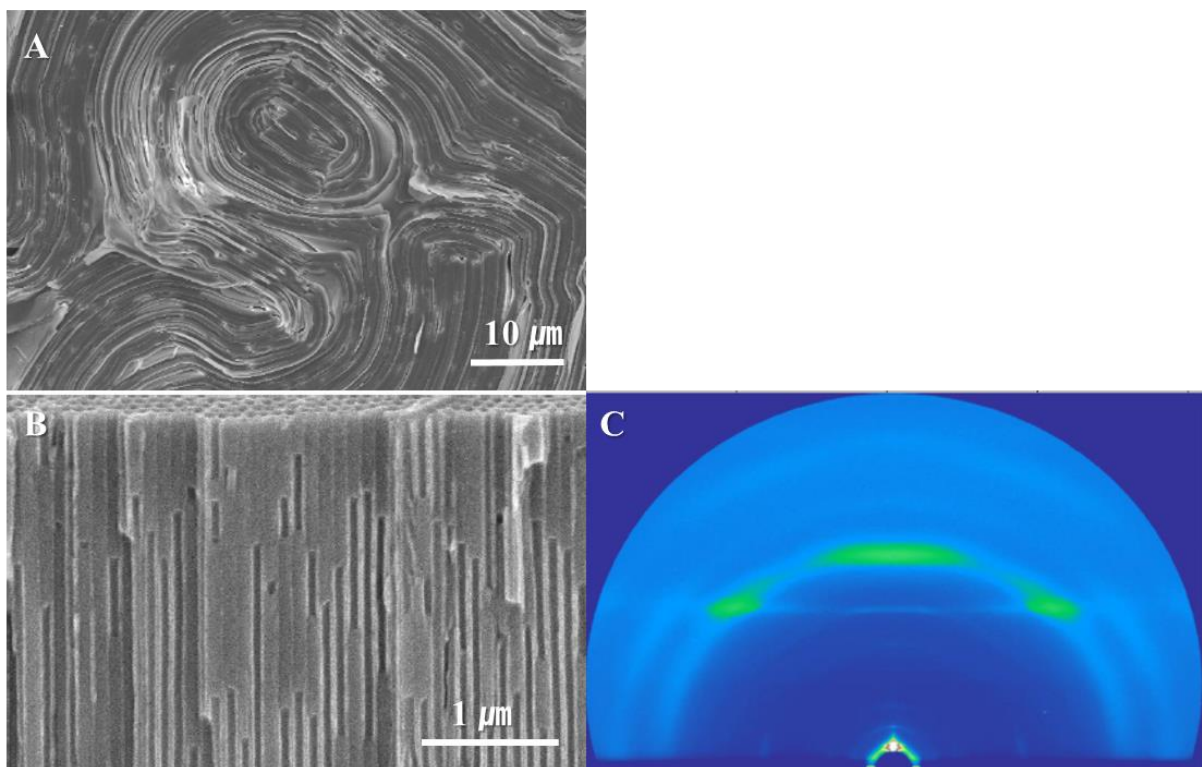
Figure 3.7 SEM images of bent-core liquid crystal. P8-O-PIMB6* (A), P9-O-PIMB7* (B), and GIXD analysis of P9-O-PIMB7* (C).

3.5 Summary

P8-O-PIMB6*, P9-O-PIMB7* and P8-O-PIMB6 were synthesized in order to observe well-defined morphology of bent-core mesogens in the 60 nm AAO nanochannel. The transition temperature of bent-core mesogens was measured by DSC. These results were similar to previous data. The morphologies

of bent-core mesogens exhibited cylindrical structure. We suppose additional chiral carbon irritates symmetry-broken molecular packing due to steric hindrance.

References

1. Hiroto, S.; Hideo, F.; Yoshiki, I.; Masahiro, K.; Hiroshi, K., Flexible Grayscale Ferroelectric Liquid Crystal Device Containing Polymer Walls and Networks. *Jpn. J. Appl. Phys.* **2002,** *41* (8R), 5302-5306.

2. Kim, J.-H.; Yoneya, M.; Yokoyama, H., Tristable nematic liquid-crystal device using micropatterned surface alignment. *Nature* **2002,** *420* (6912), 159-162.

3. Barberi, R.; Boix, M.; Durand, G., Electrically controlled surface bistability in nematic liquid crystals. *Appl. Phys. Lett.* **1989,** *55* (24), 2506-2508.

4. Moreira, M. F.; Carvalho, I. C. S.; Cao, W.; Bailey, C.; Taheri, B.; Palffy-Muhoray, P., Cholesteric liquid-crystal laser as an optic fiber-based temperature sensor. *Appl. Phys. Lett.* **2004,** *85* (14), 2691-2693.

5. Bi, X.; Hartono, D.; Yang, K.-L., Real-Time Liquid Crystal pH Sensor for Monitoring Enzymatic Activities of Penicillinase. *Adv. Funct. Mater.* **2009,** *19* (23), 3760-3765.

6. Zhang, Y.; Shi, C.; Gu, C.; Seballos, L.; Zhang, J. Z., Liquid core photonic crystal fiber sensor based on surface enhanced Raman scattering. *Appl. Phys. Lett.* **2007,** *90* (19), 193504.

7. Du, F.; Lu, Y.-Q.; Wu, S.-T., Electrically tunable liquid-crystal photonic crystal fiber. *Appl. Phys. Lett.* **2004,** *85* (12), 2181-2183.

8. Knight, J. C.; Broeng, J.; Birks, T. A.; Russell, P. S. J., Photonic Band Gap Guidance in Optical Fibers. *Science* **1998,** *282* (5393), 1476-1478.

9. Niori, T.; Sekine, T.; Watanabe, J.; Furukawa, T.; Takezoe, H., Distinct ferroelectric smectic liquid crystals consisting of banana shaped achiral molecules. *J. Mater. Chem.* **1996,** *6* (7), 1231-1233.

10. Tomoko, S.; Teruki, N.; Masato, S.; Junji, W.; Suk-Won, C.; Yoichi, T.; Hideo, T., Origin of Helix in Achiral Banana-Shaped Molecular Systems. *Jpn. J. Appl. Phys.* **1997,** *36* (10R), 6455-6463.

11. Akutagawa, T.; Matsunaga, Y.; Yasuhara, K., Mesomorphic behaviour of 1,3-phenylene bis[4-

(4-alkoxyphenyliminomethyl)benzoates] and related compounds. *Liq. Cryst.* **1994,** *17* (5), 659-666.

12. Weissflog, W.; Lischka, C.; Benne, I.; Scharf, T.; Pelzl, G.; Diele, S.; Kruth, H. In *new banana-shaped mesogens*, *Proc. SPIE: Int. Soc. Opt. Eng.* **1998**, 3319, 14-19.

13. Diele, S.; Grande, S.; Kruth, H.; Lischka, C. H.; Pelzl, G.; Weissflog, W.; Wirth, I., Structure and properties of liquid crystalline phases formed by achiral banana-shaped molecules. *Ferroelectrics* **1998,** *212* (1), 169-177.

14. Pelzl, G., Structural and electro-optical investigations of the smectic phase of chlorine-substituted banana-shaped compounds. *Liquid Crystals* **1999,** *26* (3), 401-413.

15. Weissflog, W.; Shreenivasa Murthy, H. N.; Diele, S.; Pelzl, G., Relationships between molecular structure and physical properties in bent-core mesogens. *Phil. Trans. R. Soc. A* **2006,** *364* (1847), 2657-2679.

16. Shen, D.; Pegenau, A.; Diele, S.; Wirth, I.; Tschierske, C., Molecular Design of Nonchiral Bent-Core Liquid Crystals with Antiferroelectric Properties. *J. Am. Chem. Soc.* **2000,** *122* (8), 1593-1601.

17. Nadasi, H.; Weissflog, W.; Eremin, A.; Pelzl, G.; Diele, S.; Das, B.; Grande, S., Ferroelectric and antiferroelectric "banana phases" of new fluorinated five-ring bent-core mesogens. *J. Mater. Chem.* **2002,** *12* (5), 1316-1324.

18. Gorecka, E.; Pociecha, D.; Araoka, F.; Link, D. R.; Nakata, M.; Thisayukta, J.; Takanishi, Y.; Ishikawa, K.; Watanabe, J.; Takezoe, H., Ferroelectric phases in a chiral bent-core smectic liquid crystal: Dielectric and optical second-harmonic generation measurements. *Phys. Rev. E* **2000,** *62* (4), R4524-R4527.

19. Hough, L. E.; Jung, H. T.; Krüerke, D.; Heberling, M. S.; Nakata, M.; Jones, C. D.; Chen, D.; Link, D. R.; Zasadzinski, J.; Heppke, G.; Rabe, J. P.; Stocker, W.; Körblova, E.; Walba, D. M.; Glaser, M. A.; Clark, N. A., Helical Nanofilament Phases. *Science* **2009,** *325* (5939), 456-460.

20. Link, D. R.; Natale, G.; Shao, R.; Maclennan, J. E.; Clark, N. A.; Körblova, E.; Walba, D. M., Spontaneous Formation of Macroscopic Chiral Domains in a Fluid Smectic Phase of Achiral Molecules. *Science* **1997,** *278* (5345), 1924-1927.

21. Nakata, M.; Link, D. R.; Araoka, F.; Thisayukta, J.; Takanishi, Y.; Ishikawa, K.; Watanabe, J.; Takezoe, H., A racemic layer structure in a chiral bent-core ferroelectric liquid crystal. *Liq.*

Cryst. **2001,** *28* (9), 1301-1308.

22. Lee, S.; Kim, H.; Shin, T. J.; Tsai, E.; Richardson, J. M.; Korblova, E.; Walba, D. M.; Clark, N. A.; Lee, S. B.; Yoon, D. K., Physico-chemical confinement of helical nanofilaments. *Soft Matter* **2015,** *11* (18), 3653-3659.

23. Pelzl, G.; Diele, S.; Weissflog, W., Banana-Shaped Compounds—A New Field of Liquid Crystals. *Adv. Mater.* **1999,** *11* (9), 707-724.